ADVANCED MATERIALS
www.advmat.de

Flexible Nanogenerators for Energy Harvesting and Self-Powered Electronics

*Feng Ru Fan, Wei Tang, and Zhong Lin Wang**

Flexible nanogenerators that efficiently convert mechanical energy into electrical energy have been extensively studied because of their great potential for driving low-power personal electronics and self-powered sensors. Integration of flexibility and stretchability to nanogenerator has important research significance that enables applications in flexible/stretchable electronics, organic optoelectronics, and wearable electronics. Progress in nanogenerators for mechanical energy harvesting is reviewed, mainly including two key technologies: flexible piezoelectric nanogenerators (PENGs) and flexible triboelectric nanogenerators (TENGs). By means of material classification, various approaches of PENGs based on ZnO nanowires, lead zirconate titanate (PZT), poly(vinylidene fluoride) (PVDF), 2D materials, and composite materials are introduced. For flexible TENG, its structural designs and factors determining its output performance are discussed, as well as its integration, fabrication and applications. The latest representative achievements regarding the hybrid nanogenerator are also summarized. Finally, some perspectives and challenges in this field are discussed.

1. Introduction

A notable technological trend in today's society is the rapid growth of mobile and portable electronics for applications in communication, personal health care, and environmental monitoring. The development of renewable, portable and sustainable energy sources is of great significance for sustainable economic growth and the enhancement of our quality of life. New technology that can harvest energy by applying nanomaterials and nanotechnology from the environment as sustained, self-sufficient power sources constitute the burgeoning field of nanoenergy, which can be used for powering electronic devices.[1–5] There are many forms of energy sources that can be collected and utilized in the surrounding environment, such as solar energy, mechanical energy, thermal energy, chemical and biological energy, etc. Among these energy sources, mechanical energy may be the most widely distributed that is ubiquitously available and is specialized for human motion-related applications. It exists abundantly as different forms and is frequently located in our local environment, but the vast majority is ignored and wasted, such as human motion, walking, mechanical triggering, vibration, wind, flowing water and so forth. After the first ZnO nanowire-based nanogenerator (NG) was demonstrated in 2006,[6] various nanogenerators with different structures and functions have been developed for the efficient conversion of mechanical energy into electricity primarily through the use of two effects: piezoelectricity and triboelectricity.[7–16] As of now for the triboelectric nanogenerator (TENG), the area power density of a single nanogenerator (NG) device reaches 500 W m^{-2},[17] volume power density reaches 15 MW m^{-3},[17] and an instantaneous conversion efficiency of ≈70% has been demonstrated.[18] The tremendous output of the TENG makes it possible not only for common electronic devices but also for harvesting large scale energy derived from wind and ocean wave.[19–22]

In addition to high output performance, another outstanding feature of NG technology is its simplistic and diverse structural properties that can be applied for flexible and stretchable electronics. Flexible electronics are attracting substantial attention because of their promising applications in many areas, such as wearable electronics, bendable displays, and bioinspire artificial skins.[23–30] The realization of fully flexible electronics demands to have an appropriate flexible power supply device.[31–35] Moreover, such devices should possess the ability to be bent, folded, twisted, and stretched, but also maintain the original electronic and structural properties. Therefore, the establishment of a practical flexible energy harvesting and storage system becomes an ideal choice. The key challenge for flexible energy harvesting devices is to choose the suitable materials with good flexibility and mechanical stability, as well as design and fabricate a fully flexible structure. In the past decade, tremendous efforts have been committed to improving the performance of flexible NG in order to broaden its breadth of applications.

Here, this review focuses on the recent developments of flexible energy harvesting techniques, of which include flexible piezoelectric nanogenerators (PENGs), flexible triboelectric nanogenerators, and flexible hybrid nanogenerators (FHNGs). **Figure 1** illustrates the theme of this article and several typical

Dr. F. R. Fan, Dr. W. Tang, Prof. Z. L. Wang
Beijing Institute of Nanoenergy and Nanosystems
Chinese Academy of Sciences
Beijing 100083, China
E-mail: zlwang@gatech.edu
Prof. Z. L. Wang
School of Material Science and Engineering
Georgia Institute of Technology
Atlanta, GA 30332, USA

DOI: 10.1002/adma.201504299

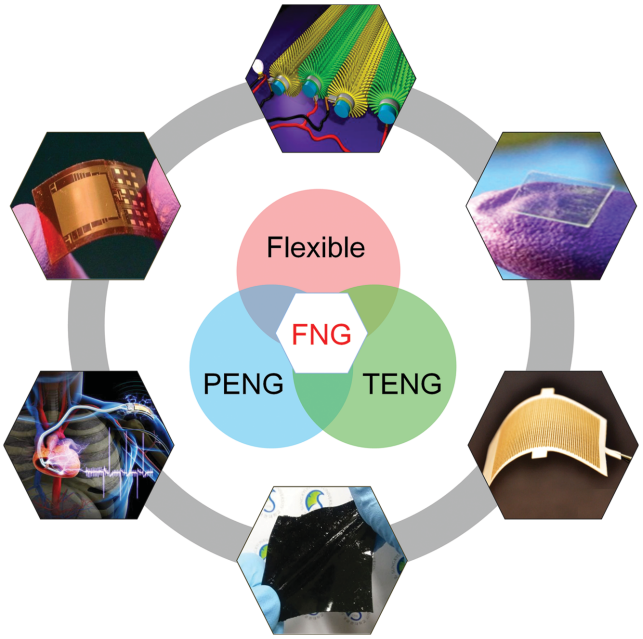

Figure 1. Schematic diagram showing the main topics of this review. Flexible NGs are based upon the coupling of flexible electronics and piezoelectric, triboelectric, and hybrid NGs. Upper left panel: Reproduced with permission.[36] Copyright 2010, American Chemical Society. Upper right panel: Reproduced with permission.[37] Copyright 2014, American Chemical Society. Lower right panel: Reproduced with permission.[38] Copyright 2015, American Chemical Society. Bottom panel: Reproduced with permission.[39] Copyright 2012, Wiley-VCH. Lower left panel: Reproduced with permission.[40] Copyright 2012, Wiley-VCH. Top panel: Reproduced with permission.[41] Copyright 2008, Nature Publishing Group.

examples of designed NGs for flexible electronics, wearable electronics, implantable electronics, and self-powered sensors. In the first segment of the review, we summarize the basic principles and the successful approaches taken for PENGs based on ZnO nanowires, conventional piezoelectric materials (lead zirconate titanate (PZT), poly(vinylidene fluoride) (PVDF), 2D materials and so on), composite materials and structures, and a performance comparison and some basic applications for powering electronic devices. In the subsequent sections, we primarily devote to elaborating on the latest progress of TENG devices in terms of its viability as a new energy technology and its application for self-powered sensors. More importantly, the emphasis of this section will be to gain an in-depth understanding of the structural design and influence of several factors on the output performance of the device. Lastly, we briefly introduce some new developments in hybrid nanogenerators based upon the integration and coupling of multiple generator modes. Some perspectives and opportunities for future development and applications of flexible nanogenerators are also discussed to conclude the review.

2. Flexible Piezoelectric Nanogenerator

2.1. Piezoelectricity and Mechanism

Harvesting of mechanical energy by piezoelectric nanogenerators (PENGs) has received a great amount of attention because of its diverse flexibility of its sophisticated design to directly convert mechanical energy into electricity for many integrated applications. The fundamental of electricity generation

Feng Ru Fan received his BS (2006) and PhD degree (2013) in Physical Chemistry from Xiamen University in China, under the joint direction of Prof. Zhongqun Tian and Prof. Zhong Lin Wang. From 2008 to 2011, he pursued a visiting study in Zhong Lin Wang's group at Georgia Institute of Technology. His research focuses primarily on nanogenerators and self-powered systems, active sensors, and the synthesis and applications of functional nanomaterials.

Wei Tang is an associate professor at the Beijing Institute of Nanoenergy and Nanosystems, Chinese Academy of Sciences. He received his BS and PhD degree from the School of Physics and the School of Electronics Engineering and Computer Science, in 2008 and 2013, respectively, from Peking University, China. After graduation, he worked in Beijing Institute of Nanoenergy and Nanosystems as a postdoctoral research fellow. His research interests include micro/nanoengineering, triboelectric nanagenerators, self-powered micro/nanosystems, and wireless sensing networks.

Zhong Lin(ZL) Wang is the Hightower Chair in Materials Science and Engineering and Regents' Professor at Georgia Tech. He is also the chief scientist and director of the Beijing Institute of Nanoenergy and Nanosystems, Chinese Academy of Sciences. His discovery and breakthroughs in developing nanogenerators and self-powered nanosystems establish the principle and technological road map for harvesting mechanical energy from environmental and biological systems for powering personal electronics and future sensor networks. He coined and pioneered the field of piezotronics and piezophototronics.

Adv. Mater. **2016**,
DOI: 10.1002/adma.201504299

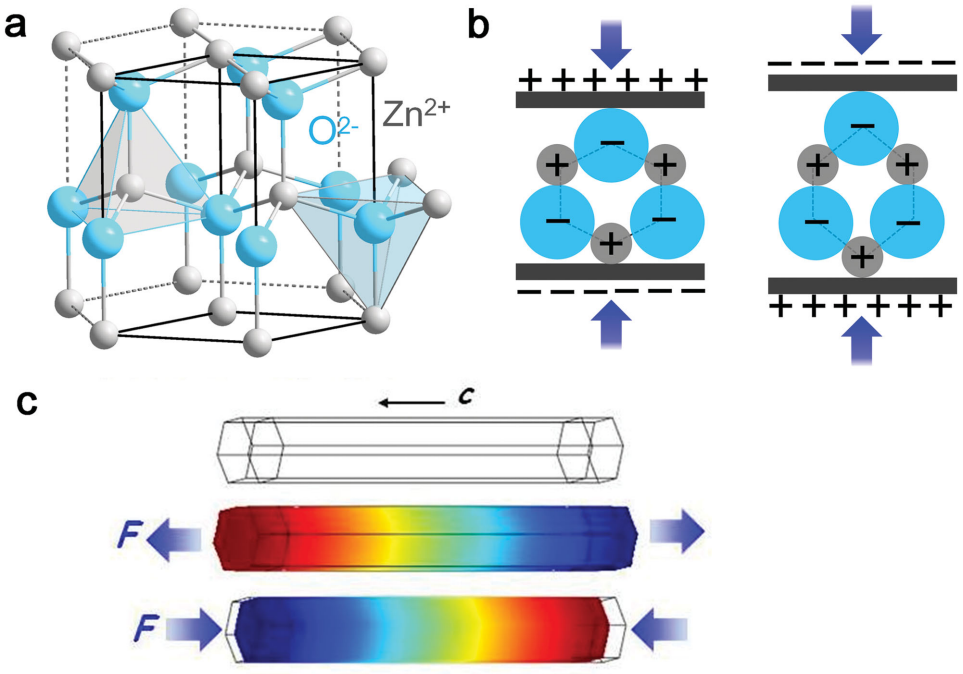

Figure 2. a) Atomic model of the wurtzite-structured ZnO. b) Piezoelectric properties and the different piezopotential in tension and compression modes of the material. c) Numerical calculation of the piezoelectric potential distribution in a ZnO nanowire under axial strain. c) Reproduced with permission.[42] Copyright 2009, AIP Publishing LLC.

in piezoelectric materials is the breaking of central symmetry in the crystal structure under external force, thereby forming a piezoelectric potential, or piezopotential. For example, when the wurtzite-structured ZnO crystal is implemented as the modular material system, the tetrahedrally coordinated Zn^{2+} and O^{2-} are stacked layer-by-layer along the *c*-axis (see **Figure 2**a). The charge center of the cations and anions coincide with one another at its undisturbed state. The structure is deformed when an external force is applied. Therefore, the charge centers of the cations and anions are separated and form an electric dipole, resulting in the formation of a piezopotential (Figure 2b). For a deformed crystal connected to an external load, the free electrons are driven to flow through the external circuit in order to partially screen the piezopotential and achieve a new equilibrium state, which is the energy conversion process (see Figure 2c).[42] Therefore, the principle of the nanogenerator is a steady stream of pulse current flowing through the external circuit if the piezopotential is continuously changed by applying a dynamic straining phenomenon.[9] The basic principle and model of power generation applies to other PENGs based on various piezoelectric materials, such as PZT, $BaTiO_3$ (BTO) and PVDF. PENGs are based on the coupling of piezoelectric materials and flexible substrates. Material selection and structural design are the core factors for the development of PENG.

2.2. PENGs Based on ZnO Nanowires

2.2.1. Lateral ZnO Nanowires

Figure 3a shows that a piezoelectric ZnO nanowire is fixed at both ends to electrodes and laterally packaged on a flexible substrate.[43] The bending of the substrate induces a uniaxial tensile strain in the ZnO nanowire, resulting in a piezoelectric potential along the wire that drives electrons to flow along the external circuit. A repeated bending-releasing process of ZnO nanowire (NW)-based PENG outputs a pulse alternating current signal. The generated open-circuit voltage and short-circuit current are 20–50 mV and 400–750 pA, respectively. (see Figure 3b). This approach provides a new methodology for harvesting biomechanical energy into electricity, for example the finger movement, the running of a hamster, or the heartbeat of a rabbit, even if the motion is irregular with mechanical instability and fluctuation.[44,45] For realistic applications, it is essential to enhance the output power of PENG by integrating large numbers of nanowires in a parallel configuration on a single flexible platform. Accordingly, a multiple lateral-nanowire-array based flexible nanogenerator was fabricated by integrating 700 rows with each row containing ≈20 000 lateral ZnO NWs (Figure 3c).[46] The whole device exhibits adequate flexibility and the nanowires are robust to prevent mechanical deformation (Figure 3d). When the device was periodically deformed, a maximum voltage of 1.26 V and a maximum current of 28.8 nA was achieved.

Highly integrated ZnO NWs are possible for fabricating flexible energy harvesters that possess a higher output to directly power applicable electronic devices. Zhu et al. demonstrated a high-output PENG based on a lateral ZnO NW array by utilizing a sweeping-printing method.[36] Firstly, the vertically-aligned ZnO NWs were transferred to a flexible substrate to form horizontally-aligned arrays with a crystallographic alignment. Then, metal electrodes were deposited by conventional photolithographic procedures to connect the NWs together (Figure 3e,f). The same growth and alignment direction of NWs

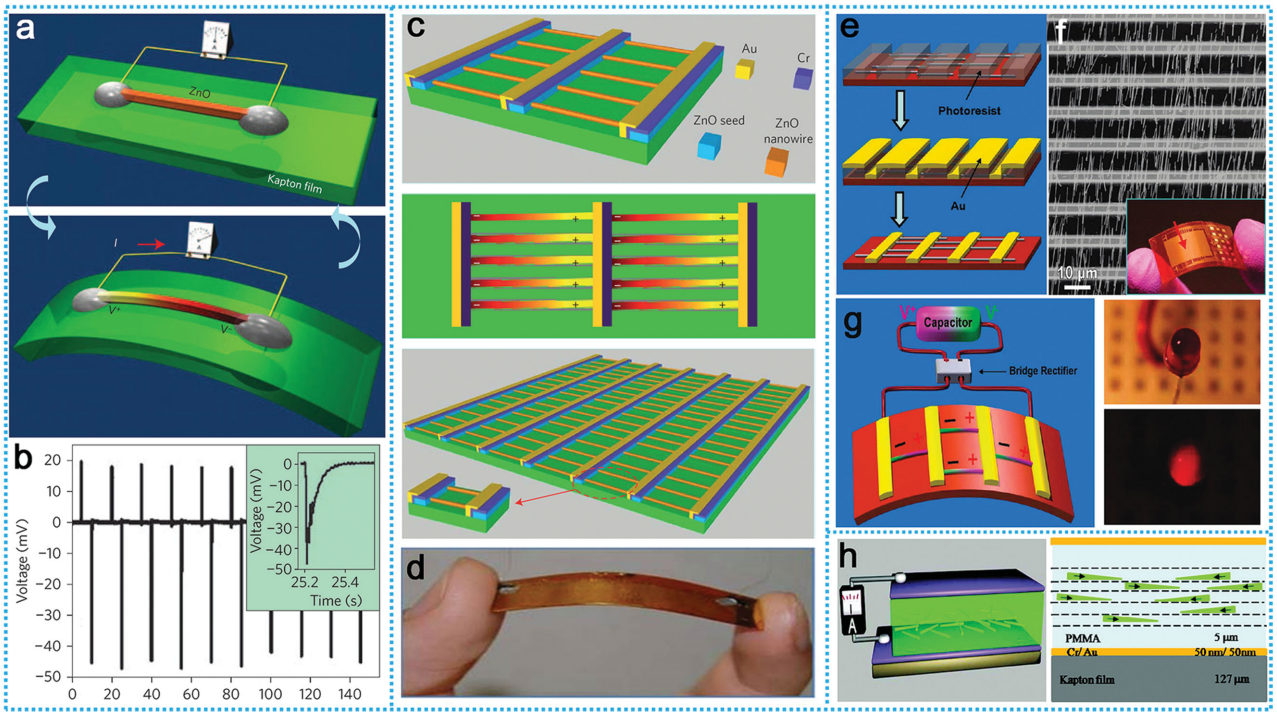

Figure 3. Flexible PENGs based upon horizontal ZnO NW arrays. a,b) Design of a single piezoelectric wire generator on a flexible substrate. Mechanical bending of the substrate generates piezopotential to drive electrons through the external circuit. Reproduced with permission.[43] Copyright 2009, Nature Publishing Group. c,d) Structure and optical images of a flexible lateral-nanowire-array integrated NG. Reproduced with permission.[46] Copyright 2010, Nature Publishing Group. e–g) Fabrication process and output performance characterization of a flexible NG based upon a lateral ZnO NW array. Reproduced with permission.[36] Copyright 2010, American Chemical Society. h) Flexible NG fabricated by rational unipolar assembly of conical ZnO NWs. Reproduced with permission.[47] Copyright 2010, American Chemical Society.

guarantees the consistency of the piezoelectric potentials and a successful scaling up of the output performance. In this report, an open-circuit voltage was up to 2.03 V and a peak output power density was ≈11 mW cm^{-3}. Furthermore, the electricity generated by the PENG can be effectively stored into capacitors and utilized to power a commercial light-emitting diode (LED), demonstrating great potential for application in electronic devices (Figure 3g). However, the photolithographic fabrication method is a very technical and complex process, limiting the potential of PENGs for scale-up to meet industrial demands. To address this problem and to improve the energy output performance, Hu et al. fabricated a new PENG based on a composite structure by simply dispersing conical ZnO NWs onto a flat polymer film, as illustrated in Figure 3h.[47] Due to the piezoelectric potential superposition of each conical NW, the device generates a macroscopic induced potential difference between top and bottom electrodes due to mechanical deformation. The output was measured to be 2 V in voltage and 50 nA in current, which can continuously drive the small commercial electronics, such as liquid crystal displays (LCDs). This flexible PENG is simple, cost-effective, and scalable technology for small personal electronics and self-powered systems.

2.2.2. Vertical ZnO Nanowires

As previously mentioned, mechanical energy can be converted into electrical energy by means of lateral ZnO nanowires and assembled arrays. Similarly, the as-grown vertical ZnO NWs aligned along the *c*-axis have consistent polar directions and can be used to fabricate high output PENGs. A unique advantage for solution-based growth of vertical ZnO NW arrays is that they can be grown at 80 °C on substrates of any shape and any material.[48,49] After sputtering a seed layer on the substrate, well-aligned NWs can be easily grown on this layer to form a quasicontinuous film using a simple growth technique. This fabrication technique is a simple, low-cost, and large-scale approach for a broad range of applications. A large number of flexible substrates can be used for growing ZnO NW arrays that will benefit the design of various structures and types of PENGs for flexible and portable electronics. In 2009, Choi et al. fabricated a fully flexible and transparent piezoelectric NG based on vertically-aligned ZnO NWs.[50] The basic principle pertains to the previous direct-current (DC) NG that a Schottky barrier at the interface between ZnO NWs and the metal electrode controls the flow of electrons generated by the piezoelectric potential. However, as a flexible device, it has a few shortcomings in terms of the mechanical durability of the electrodes that are detrimental to the device's lifetime and performance stability. To resolve this problem, this research group developed a PENG using conductive single-walled carbon nanotube (CNT) network sheets as the contact electrodes.[51] The output current density was significantly enhanced due to the improved contact and low resistance variation, while the device exhibited exceptional durability and stability.

Adv. Mater. **2016**,
DOI: 10.1002/adma.201504299

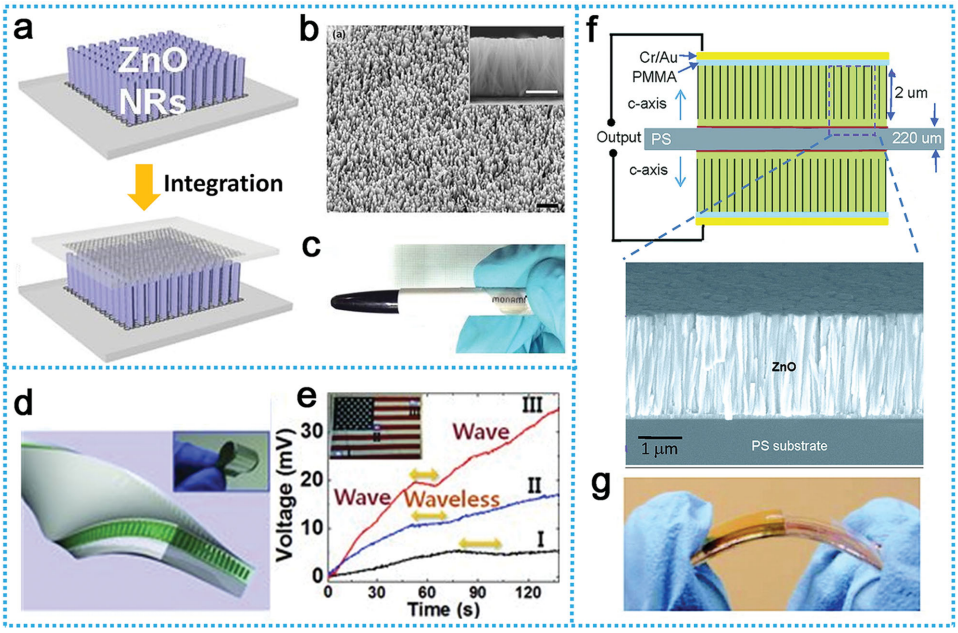

Figure 4. Flexible PENG based on vertical ZnO NW arrays. a–c) Integrated fully rollable NG prepared by growing ZnO NW arrays on graphene substrate. Reproduced with permission.[54] Copyright 2010, Wiley-VCH. d,e) High-output NG made of a free cantilever beam that consisted of a multi-layer structure. The bending of the device shows its good mechanical flexibility. Reproduced with permission.[55] Copyright 2011, American Chemical Society. f,g) Super-flexible NG based on ultrathin Al foil being utilized as an active deformation sensor to monitor the waving motion of a flag. Reproduced with permission.[56] Copyright 2013, Wiley-VCH.

In comparison with other electrode materials, graphene possesses extraordinary electrical and mechanical properties, which has attracted substantial interest in its application for flexible electronics.[52,53] Combining the features of graphene and the piezoelectricity of ZnO NWs, Choi et al. developed a fully rollable, transparent NG consisting of ZnO NWs grown epitaxially on a 2D graphene electrode using the conventional solution growth method (**Figure 4**a–c).[54] The output current density was about 2 μA cm^{-2} and demonstrated no fluctuations after the device was rolled several times on a pen. Such stable and reliable output performance is due to the mechanical and structural strength of the graphene-based PENG that behaves with superior charge-scavenging performance at the electrode interfaces.

Unlike the aforementioned direct-current PENGs, Hu et al. reported a new alternating-current PENG based on vertical ZnO NW arrays.[55] The most striking difference is that a thin layer of poly(methyl methacrylate) (PMMA) was coated on top of the ZnO film to serve as an insulating layer, and then deposited a metal electrode (Figure 4d,e). By the coupling of piezoelectric potential and electrostatic induction, a cycling mechanical deformation of the device results in the back-and-forth flow of electrons through the external load. The measured output voltage was ≈20 V and the output current was over 8 μA (corresponding to an ideal maximum power density of 0.16 W cm^{-3}). Based on the same principle, Lee et al. developed a super-flexible NG using a thin Al foil at a thickness of ≈18 μm as the substrate and electrode.[56] As shown in Figure 4f,g, this PENG can harvest the energy from a waving flag, demonstrating its superior flexibility, which can be integrated into fabric-based applications. The device can also be applied as an active sensor to detect the wrinkling of a human face. Under the blinking motion, the output voltage and current were measured to be about 0.2 V and 2 nA, respectively. Furthermore, PENGs based on a thin Al substrate can be easily integrated into a multilayer structure without size and number restrictions.[57] Simplified integration of NGs in parallel and series configurations will clearly enhance the output performance of the overall device. Under the conditions of a human walking, the maximum output voltage and current reached up to 3.2 V and 195 nA, respectively.

2.2.3. ZnO Fiber Structures

ZnO NW-based PENGs can be fabricated on a variety of flexible substrates, such as metals, polymers, and even on arbitrarily curved substrates (i.e., fiber). A fiber-based PENG has been fabricated for converting vibration or mechanical energy into electricity using piezoelectric ZnO NWs radially grown around textile fibers (**Figure 5**a,b).[41] The whole structure of the device can be seen as "brush-to-brush", in other words, one brush is made of ZnO nanowires is one brush as well as the metal nanowires is another one. A cycled relative sliding motion between the two fibers produces power output owing to the deflection and bending of the ZnO nanowires (Figure 5c). This prototype of fiber-based PENG shows its distinct advantages in the building of a flexible, adaptable, and wearable power source that establishes the foundation for smart clothing applications. Lee et al. developed a hybrid-fiber piezoelectric generator composed of ZnO NWs and poly (vinylidene fluoride) (PVDF) polymer coating a conducting fiber to convert low-frequency

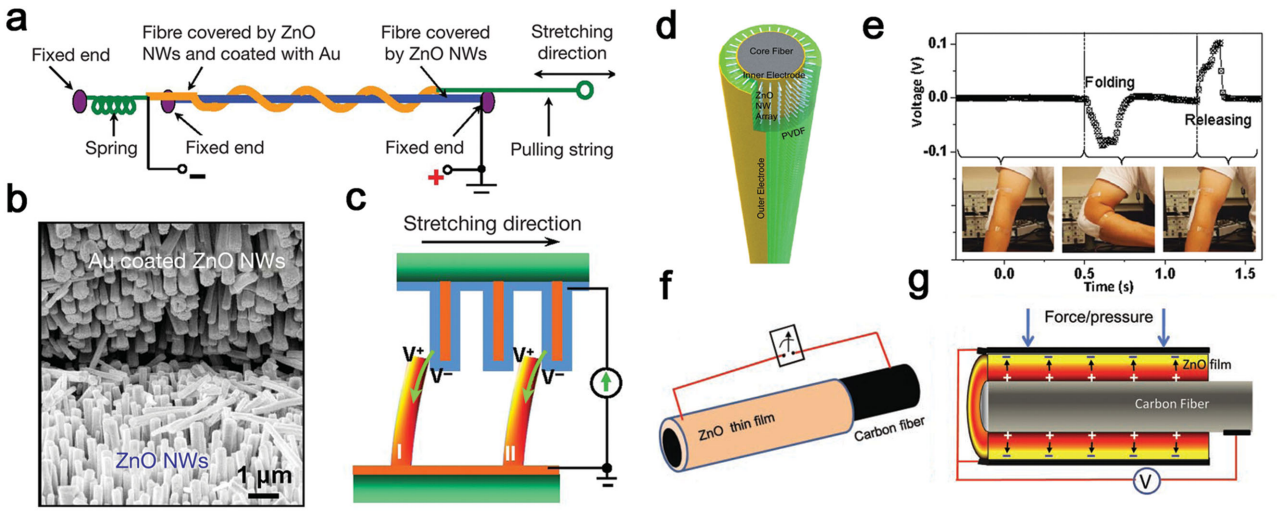

Figure 5. Schematic illustration of the ZnO fiber-based PENGs. a–c) Experimental setup, internal structure, and mechanism of PENG fabricated by ZnO NWs grown radially around textile fibers. Reproduced with permission.[41] Copyright 2008, Nature Publishing Group. d,e) Structure of a hybrid-fiber NG consists of ZnO NWs and PVDF film, and electrical measurements of a device attached on a human elbow. Reproduced with permission.[58] Copyright 2012, Wiley-VCH. f,g) Fiber NG and active sensor based on ZnO film formed on the surface of a carbon fiber. Reproduced with permission.[59] Copyright 2011, Wiley-VCH.

(<1 Hz) mechanical energy into usable electricity.[58] By attaching this PENG device on a human arm, the folding-releasing motion of the elbow produces an output voltage, current density and power density of 0.1 V, 10 nA cm^{-2} and 16 μW cm^{-3}, respectively (Figure 5d,e). This approach shows high performance and feasibility as a power source for wearable electronics. Similarly, Li et al. fabricated a flexible, fiber nanogenerator based on carbon fibers that are cylindrically covered by textured ZnO thin films.[59] As shown in Figure 5f,g, once subjected to uni-compression under an applied pressure, the ZnO thin film generates a macroscopic piezopotential across its inner and exterior surfaces, driving an electric current in the external load. Using such a device, an output peak voltage of 3.2 V and average current density of 0.15 μA cm^{-2} are demonstrated. Because of its outstanding performance, this PENG can serve as a promising option for ultrasensitive sensors to monitor the behavior of the human heart, which one could envision being applied to medical diagnostics as sensors and measurement tools. To date, a variety of flexible energy harvesters based on the fiber structure have been developed and they can be used to harvest mechanical movement induced by the human body or an air flow for the power generation or sensing applications.[60–64]

2.3. PENGs Based on Other Piezoelectric Materials

2.3.1. PZT-Based PENGs

PZT is a widely used piezoelectric ceramic material with high dielectric constants and piezoelectric voltage, which are ideal properties for the materials required to convert mechanical to electricity.[65–67] However, due to the brittle nature of a thin film, PZT materials cannot withstand flexible and stretchable operation modes. The maximum safe strain for PZT is 0.2% and is indicative of structural failure under even a slight amount of stretching. To overcome this undesirable attribute, researchers have proposed various innovative designs of NGs based on the different morphology and properties of PZT. Qi et al. transferred highly crystalline piezoelectric PZT nanoribbons in high yields and over large areas onto rubber or plastic films for flexible energy harvesting using a scalable transfer printing method.[68] As illustrated in **Figure 6**a,b, crystalline PZT ribbons were grown on an MgO substrate using a standard RF-sputtering method. Then, the substrate was undercut etched and the separated PZT nanoribbons were transfer printed onto flexible polydimethylsiloxane (PDMS) rubber. The fundamental piezoelectric properties of the ribbons characterized via piezo-force microscopy indicates that their piezoelectric charge constants (d_{31} = 79 pm V^{-1}, d_{33} = 101.0 pm V^{-1}) is one of the highest record on a flexible substrate. A small PENG (1 cm × 1 cm area), prepared with printed PZT piezoelectric ribbons, has generated the maximum values of current and voltage output of 40 nA and 0.25 V, respectively, at a tapping frequency of 3.2 Hz. On the basis of this work, Qi et al. fashioned the PZT ribbons into a wavy shape pattern and integrated them with stretchable PDMS rubber to withstand large amounts of elastic strain.[69] As shown in Figure 6c,d, a slab of PDMS was elastically stretched and brought into conformal contact with the ribbons and released the strain to form PZT wavy/buckled ribbons. The prepared device can be stretched up to 8% strain and integrated into flexible NG devices. A PENG consisting of 10 ribbons produced a current output of 60 pA, corresponding to a current density of 2.5 μA mm^{-2}, which favorably compares to the peak current density measured in PZT nanowire-based devices.

Park et al. introduced a highly-efficient, flexible, and large-area PZT thin film based NG synthesized via a laser lift-off (LLO) process.[70] By laser irradiation, the entire area of the PZT thin film can be transferred onto a flexible substrate without causing structural damage (Figure 6e,f). During periodical bending-releasing process, the measured output voltage and current signals reached up to ≈200 V and 150 μA cm^{-2},

DOI: 10.1002/adma.201504299

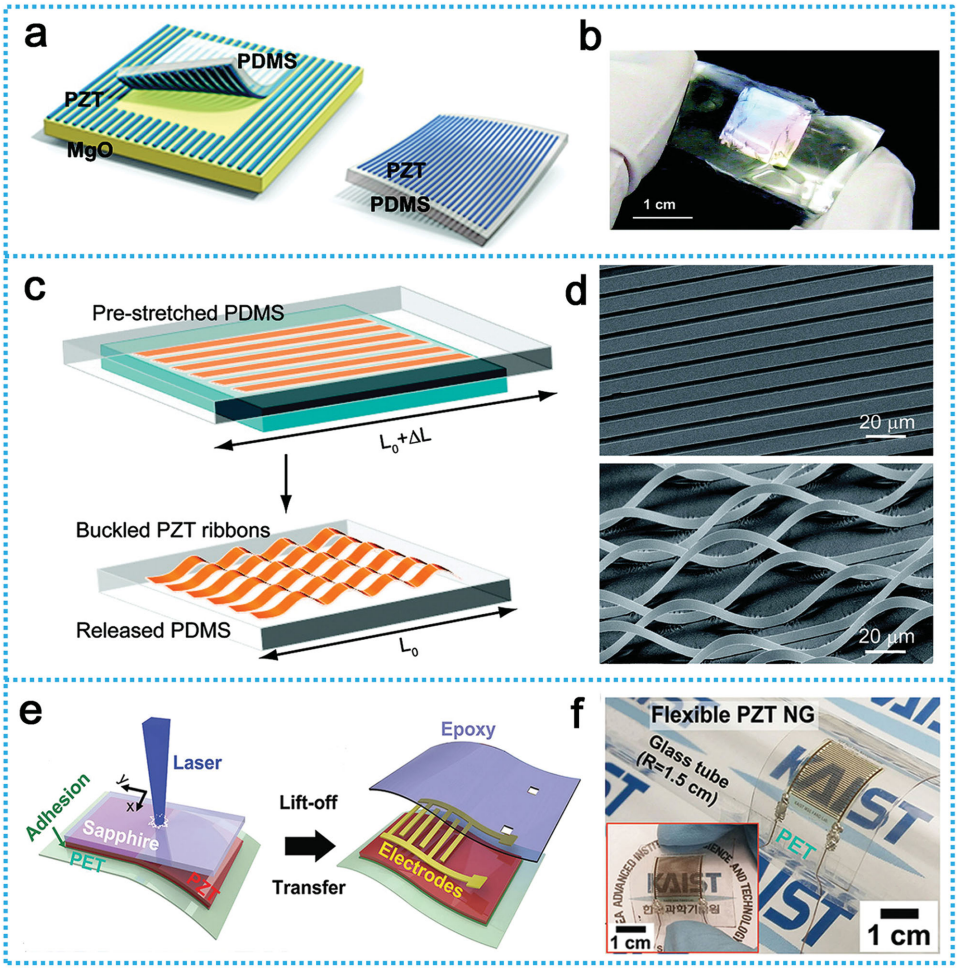

Figure 6. a–c) Schematic diagram and optical microscopy image of crystalline PZT ribbons on a flexible PDMS substrate. Reproduced with permission.[68] Copyright 2012, American Chemical Society. c,d) Formation and SEM images of wavy/buckled piezoelectric PZT ribbons via a prestretched method. Reproduced with permission.[69] Copyright 2011, American Chemical Society e,f) Fabrication process and image of a flexible PZT thin film-based NG using the laser lift-off method. Reproduced with permission.[70] Copyright 2014, Wiley-VCH.

respectively. The short-circuit current generated from a large-area PZT based PENG (3.5 cm × 3.5 cm) by human finger motions reached up to ≈8 μA and was capable of directly operating over 100 blue LEDs without any external power source. Kwon et al. prepared PZT ribbon-based flexible, semi-transparent NGs implementing graphene as the interdigitated electrodes to improve the interfacial performance.[66] Electrical performance measurements demonstrated a high output voltage of ≈2 V, current density of ≈2.2 mA cm^{-2} and a power density of ≈88 mW cm^{-3} at an application force of 0.9 kgf.

In addition to nanoribbions, PZT nanofibers can be implemented to fabricate a variety of high -performance PENG devices. Chen et al. reported a high-output NG based on laterally-aligned PZT nanofibers.[71] The PZT nanofibers were prepared via electrospinning technology with a diameter of ≈60 nm and length of ≈500 μm; the measured output voltage and power under periodic stress application to the soft device was 1.63 V and 0.03 μW, respectively. Recently, Qin and co-workers prepared a high output NG device based on vertically-aligned, ultra-long PZT nanofibers fabricated via electrospinning method.[72] The integrated NG is capable of being bent, stretched, or twisted to a large degree without breaking its structure. A high output voltage of 209 V and a peak current of 53 μA corresponding to current density of 23.5 μA cm^{-2} were achieved. These flexible piezo-devices have been shown to be particularly efficient electromechanical energy converters that demonstrate a promising step toward the implementation of wearable and implantable power sources and self-powered systems.[73]

2.3.2. PVDF-Based PENGs

Polymer-based piezoelectric materials, such as PVDF or its similar copolymer P(VDF-TrFE), are commonly used for piezoelectric applications because of their advantageous properties of flexibility, adequate mechanical strength, ease of processing and high chemical resistance. Polymers' chemical stability and biocompatibility is in favor of its application in biological systems, such as implantable sensing and energy harvesting. A notable disadvantage is that achieving good performance requires

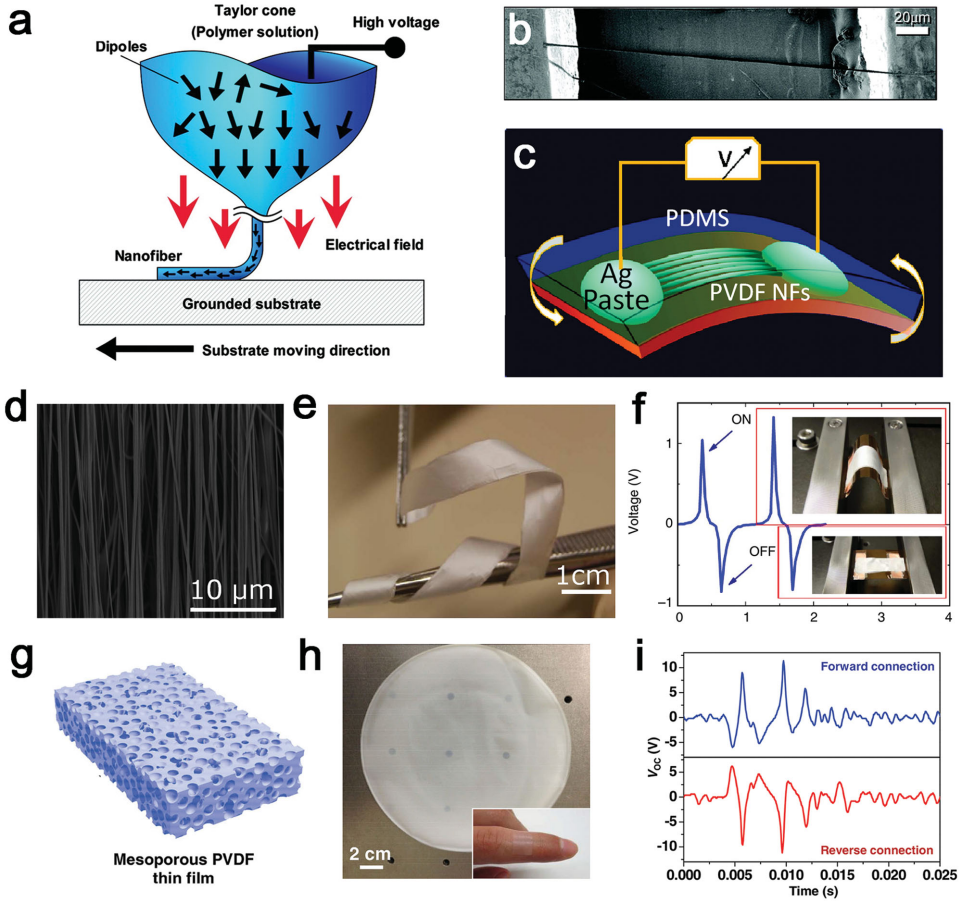

Figure 7. Flexible PENG using piezoelectric PVDF material. a–c) Schematic diagram and SEM image of poled PVDF fiber prepared via near-field electrospinning method. a–b) Reproduced with permission.[74] Copyright 2010, American Chemical Society. c) Reproduced with permission.[75] Copyright 2010, American Chemical Society. d–e) SEM micrographs and photograph of a free-standing film of highly aligned piezoelectric fibers of P(VDF-TrFe) used for PENG. Reproduced with permission.[76] Copyright 2013, Nature Publishing Group. g–i) Processing and structure of sponge-like mesoporous PVDF thin films for scalable and integratable NGs. Reproduced with permission.[79] Copyright 2014, Wiley-VCH.

electrical poling in which mechanical stretching processes need to align the dipoles of the polar β-phase of PVDF structures. A variety of strategies have been proposed for fabricating flexible polymeric piezoelectric power generators. Chang et al. have demonstrated PVDF nanogenerators that are directly written onto flexible plastic substrates utilizing a direct-write technique via near field electrospinning (NFES) (**Figure 7**a).[74] Through an in situ mechanical stretch and electrical poling process, PVDF nanofibers were fabricated under a high bias voltage (>10 kV) which allows for the transformation of nonpolar α-phase to polar b-phase for piezoelectricity. The output performance of a single PVDF nanofiber-based device (Figure 7b) was 0.5–3 nA of current and 5–30 mV of voltage under repeated long term reliability tests with negligible performance degradation. Multiple nanofibers were arranged in either serial or parallel connections to increase the total electrical output (Figure 7c).[75]

To take a step further, researchers sandwiched randomly-oriented electrospun PVDF nanofiber webs between two plate electrodes to form a vibration-driven generator. Persano et al. prepared a large area, flexible, free-standing film of highly-aligned piezoelectric P(VDF-TrFE) fibers by use of electrospinning onto a fast rotating collector (Figure 7d–f).[76] This film exhibited superior flexibility and mechanical robustness and can be repeatedly bent and folded without any damage. The current of 40 nA and voltage of 1.5 V were achieved from a fiber array-based PENG on 225 μm thick substrates at a bending frequency of 2 Hz. Because of its good piezoelectric properties, fiber array-based pressure sensors exhibit excellent response at extremely small pressure values (0.1 Pa). Other simple devices can be easily constructed that include accelerometers, orientational, and vibrometer sensors.

The aforementioned aligned PVDF fibers were primarily deposited on two electrodes adhered to a flexible substrate that requires a large bending of the device to generate a sufficient stretching of the fibers for effective energy conversion. To overcome this problem, two novel structural designs have been proposed and practiced. Chen et al. demonstrated a self-connected vertically integrated generator composed of piezoelectric P(VDF-TrFE) microfiber arrays by a patterned electrohydrodynamic (EHD) pulling method.[77] The nanogenerator is fabricated by applying a voltage to the electrode pair separated by void air space and an array of shallow micropillars, generating a

Adv. Mater. **2016**,
DOI: 10.1002/adma.201504299

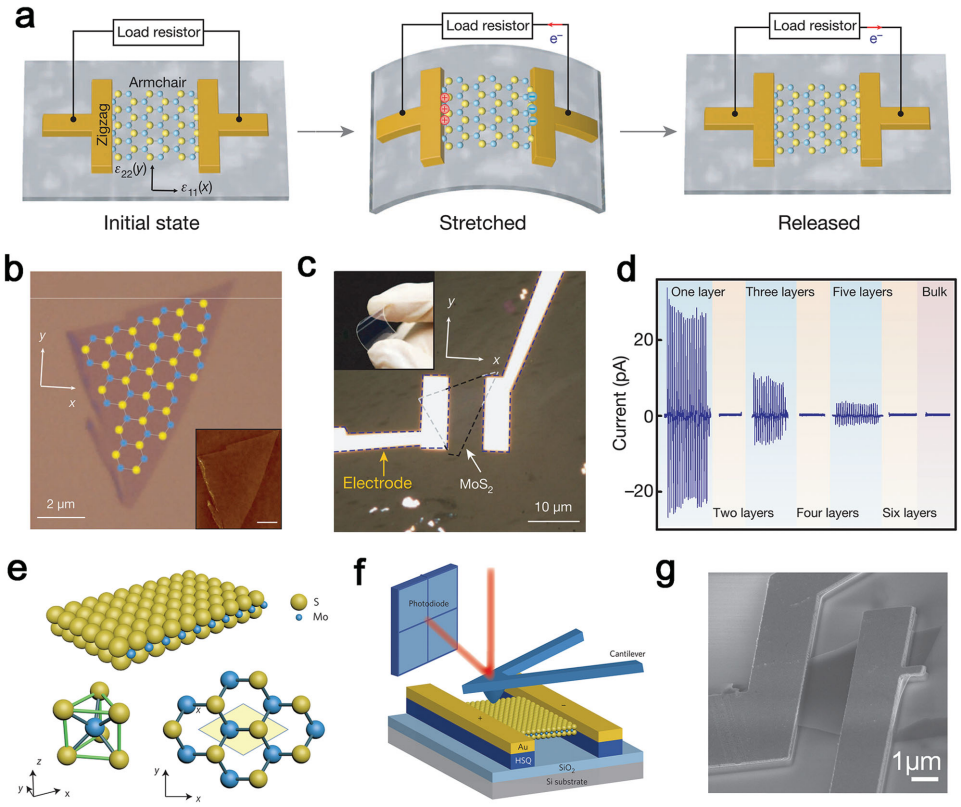

Figure 8. Flexible PENGs using a piezoelectric monolayer MoS_2. a) Operation scheme of piezoelectric NG based on the MoS_2 monolayer. b–d) Morphological and performance characterization of the flexible single-layer PENG. a–d) Reproduced with permission.[84] Copyright 2014, Nature Publishing Group. e–g) Probing the piezoelectric property of free-standing monolayer MoS_2. Reproduced with permission.[85] Copyright 2015, Nature Publishing Group.

microfiber array in robust contact with the upper electrode. This nanogenerator gives an output voltage of 4.0 V and a current of 2.6 μA, which an enhancement by a factor of 5.4 relative to the bulk film. Cha et al. created nanoporous PVDF films using ZnO nanowires as a template demonstrating an effective conversion of mechanical oscillations generated by the sonic wave to electricity.[78] PVDF nanogenerators generated the output voltage and current signals of 2.6 V and 0.6 μA, a power density of 0.17 mW cm^{-3}. Using ZnO nanoparticles as a template, Mao et al. prepared sponge-like mesoporous piezoelectric PVDF thin films possessing unique merits for fabricating highly flexible and stretchable piezoelectric devices.[79] As shown in Figure 7g–i, the mesoporous PVDF thin films in the wafer scale were translucent, soft, and very flexible, which can directly attach to the surface of human skin or an electronic device and effectively convert ambient mechanical oscillations to electricity. A typical PENG of the dimensions 2 cm × 1 cm can produce average peak values of voltage and current up to 11.0 V and 9.8 μA, respectively. Furthermore, multiple NGs can be directly integrated into one system to enhance its output without rectifying or synchronizing individual signals. In addition to ZnO, PZT and PVDF, other piezoelectric materials also enable flexible NGs to applied to different areas owing to their special properties, such as GaN,[80] and $ZnSnO_3$.[81] This technique proves to be scalable and integratable, taking a promising step for developing wearable electronics and practical self-powered electronic devices.

2.3.3. 2D Materials-Based PENGs

Recently, 2D atomic-layer materials, such as transition metal dichalcogenides (TMDs), have received significant attention owing to their unique electrical, optical and other physical and chemical properties.[82,83] In the case of MoS_2, the electron mobility is better than that of amorphous silicon and many other ultrathin semiconductors which were tested for use in futuristic applications such as roll-up displays and other flexible, stretchable electronics. Monolayer MoS_2 is predicted to exhibit piezoelectricity due to its broken inversion symmetry in crystal structure (**Figure 8**e). In a recent study by Wang and co-workers, they have made the first experimental observation of piezoelectricity and the piezoelectronic effect in an atomically thin MoS_2 flake, resulting in a transparent and flexible NG (Figure 8a–c).[84] The bending of MoS_2 flakes with odd number of layers can produce an electrical output, whereas no output is observed for flakes with an even number of layers (Figure 8d). A single-layer MoS_2 device under 0.53% strain generates a voltage of 15 mV and a current of 20 pA, corresponding to a power density of 2 mW m^{-2} and a 5.08% mechanical-to-electrical energy conversion efficiency. The piezoelectricity, large mechanical stretchability and flexibility of atomically thin MoS_2 demonstrate its potential for applications in electromechanical sensing, wearable technology, pervasive computing and implanted devices.

The existence of piezoelectricity in free-standing monolayer MoS_2 has also latterly proved by atomic force microscopy measurement.[85] When an electric field is applied across a free-standing MoS_2 monolayer, the tension of monolayer will change due to the piezoelectric effect, resulting in the deflection of a cantilever. Therefore it is can be used for the quantification of the piezoelectric responses (Figure 8f,g). Results demonstrate that monolayer MoS_2 exhibits a piezoelectric effect with a coefficient of 2.9×10^{-10} C m^{-1}, comparable to widely piezoelectric wurtzite structure materials (e.g., ZnO). Two-dimensional piezoelectric materials could enhance the piezoelectric performance through a rational design and further demonstrate the feasibility of array integration to enhance the performance of energy conversion materials.

2.4. PENGs Based on Composite Materials and Structures

Besides conventional piezoelectric materials, many other natural materials such as fibrous proteins and collagen fibrils inherently possess piezoelectric properties. However, these materials have low piezoelectric coefficients and suffer no effective way to process such materials for large-scale applications. Lee and co-workers demonstrated that the piezoelectric and liquid-crystalline properties of M13 bacteriophage (phage) can be utilized to generate electrical energy.[86] They first determined the piezoelectric properties of M13 and used genetic engineering to boosts the voltage of the virus. The self-assembled virus films of phage exhibit piezoelectric strength of 7.8 pm V^{-1}, comparable to poled lithium niobate ($LiNbO_3$) and PVDF films (**Figure 9**a,b). In Figure 9c, a virus-based piezoelectric energy generator that contains multilayer virus films sandwiched between two gold-plated electrodes is capable of generating 6 nA of current and 400 mV of potential, which is sufficient to power a LCD display. Because biotechnology techniques facilitate the large-scale production of genetically modified viruses, this achievement is ideal for small energy harvester and sensors due to its simple synthesis and environmentally benign fabrication process.

The piezoelectric properties of the M13 virus can be implemented to generate electrical energy. However, the generated electric current remains too small primarily due to the deformation being limited to a thin layer (about 100 nm thick). To further investigate the power generation of this bio-system, Jeong et al. proposed a high-performance, flexible NG device with a stable network of anisotropic $BaTiO_3$ structures using a template of M13 virus (Figure 9d).[87] By means of a biological self-assembly method, the filamentous shape of an M13 virus can form a percolated network of well-dispersed BTO nanochains, which proves to be crucial for the generation of effective piezopotential. The virus-enabled PENG shows a high output of ≈300 nA and ≈6 V, while the signals are relatively stable with no obvious attenuation of performance during the durability test (duration of 21 000 cycles). This study shows that the bioinspired approach proves

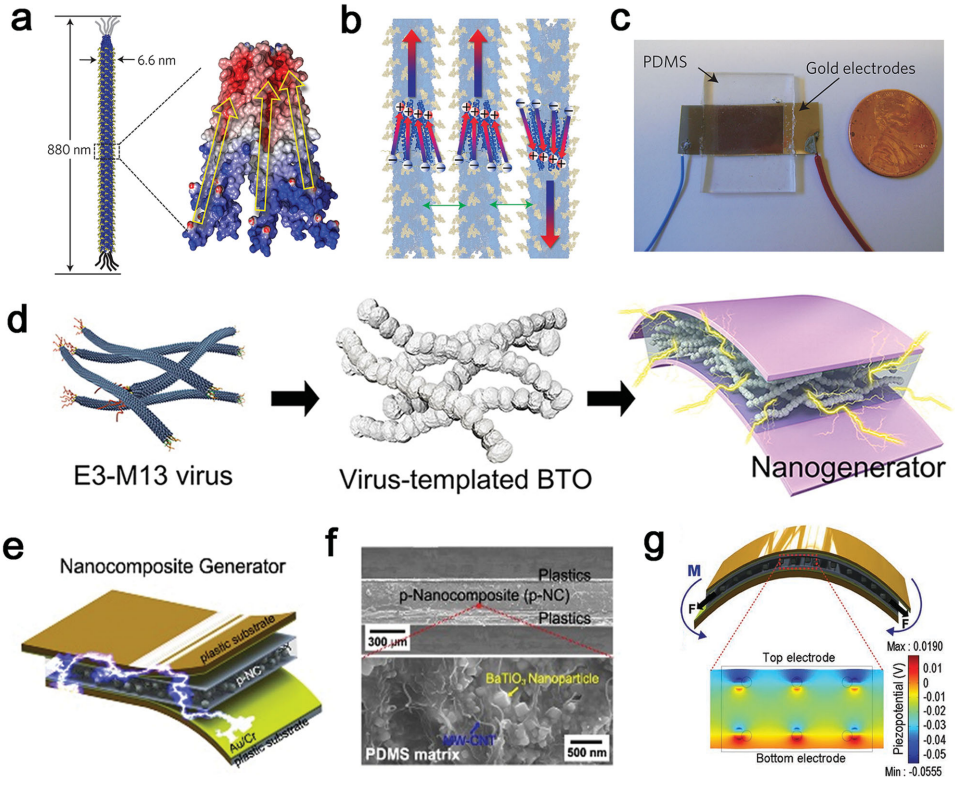

Figure 9. a–c) Schematic and photograph of virus-based piezoelectric NG. Piezoelectric monolayer phage films with randomly mixed dipoles along the axial direction. Reproduced with permission.[86] Copyright 2012, Nature Publishing Group. d) Overall fabrication process of a virus-templated BTO-based piezoelectric NG. Reproduced with permission.[87] Copyright 2013, American Chemical Society. e–g) A flexible nanocomposite generator made of BTO nanoparticles and graphitic carbon. Reproduced with permission.[88] Copyright 2012, Wiley-VCH.

Adv. Mater. **2016**,
DOI: 10.1002/adma.201504299

to be a facile method to design and fabricate nanoscale materials suitable for flexible energy harvesting applications.

Composite material-based NGs, conventionally composed of piezoelectric nanomaterials dispersed into an elastomeric matrix, are a promising option for large-scale, flexible energy harvester applications; composite-based NGs have advantageous properties, such as their facile fabrication process, cost effectiveness and mechanical robustness. The robustness and enhanced electric output broadens their potential application in consumer electronics, environmental monitoring, and sensor networks. In 2012, Park et al. reported a nanocomposite generator (NCG) fabricated by mixing BTO nanoparticles and universal graphitic carbon (i.e., CNT or reduced graphene oxide) within a PDMS matrix (Figure 9e,f).[88] The conductive carbon materials possess multiple functions that include physically dispersing, acting as a mechanical reinforcing agent and conduction pathways for electrons, which have been supported by a theoretical analysis and a finite element simulation (Figure 9g). Under continual bending and unbending cycles, the flexible NCG device repeatedly generates an open-circuit voltage of 3.2 V and short-circuit current of 350 nA. In subsequent reports, the researchers replaced BTO with additional inherent piezoelectric materials, such as PZT and alkaline niobate particles, to significantly increase the electrical output performance.[89] Flexible PZT particle-based NGs could be fabricated via spin-coating or by the Mayer bar-coating methods, as illustrated by the schematics of the overall fabrication in **Figure 10**a. A large-area PENG (30 cm × 30 cm) driven by a human hand tapping generates a maximum output voltage of up to 100 V and the current up to 10 μA. A single device can directly operate 12 commercial blue LEDs connected in series without a rectifying and storage device (Figure 10b,c).

Lee et al. realized a high-performance, flexible NG using a composite of piezoelectric single-crystal $ZnSnO_3$ nanocubes and PDMS polymer without any electrical poling process (Figure 10d).[90] A remarkable result is that their PENG generates a substantial power output under only vertical compression, yet there is negligible power generation under other forms of applied strain, such as bending and folding. For a single PENG under a rolling vehicle tire, a large recordable output voltage of about 20 V and current density of about 1 μA cm^{-2} was successfully achieved. As with other composite-based NGs, it exhibited excellent robustness and durability, while also possessing superior cyclability and stability. Besides the aforementioned nanoparticles, other composite-based NGs using various piezoelectric nanomaterials have been developed, such as $KNbO_3$,[91] $NaNbO_3$,[92] polybasic alkaline niobate,[93] P-type polymer,[94,95] and (1-x) $(Pb(Mg_{1/3}Nb_{2/3})O_3]$-x[$PbTiO_3$) (PMN-PT).[96] This kind of flexible PENG is an important and promising research branch for the flexible piezoelectric energy harvesting field since high-performance large-area NGs can be economically practical in the operation of numerous electronic devices for future applications.

The basic components needed for PENGs are flexible substrates and electrodes that can maintain their original mechanical and electrical properties after bending or stretching. Recently, a hyper-stretchable elastic-composite generator was realized by employing a rubber-based piezoelectric elastic composite with long Ag nanowire stretchable electrodes (Figure 10e–g).[97] This stretchable NG, consisting of well-dispersed PMN-PT microparticles and multi-walled carbon nanotubes (MWCNTs) with a PDMS matrix, generated outstanding power output (4 V and 500 nA) and exceptional stretchability of 200%. Under various mechanical deformations, such as

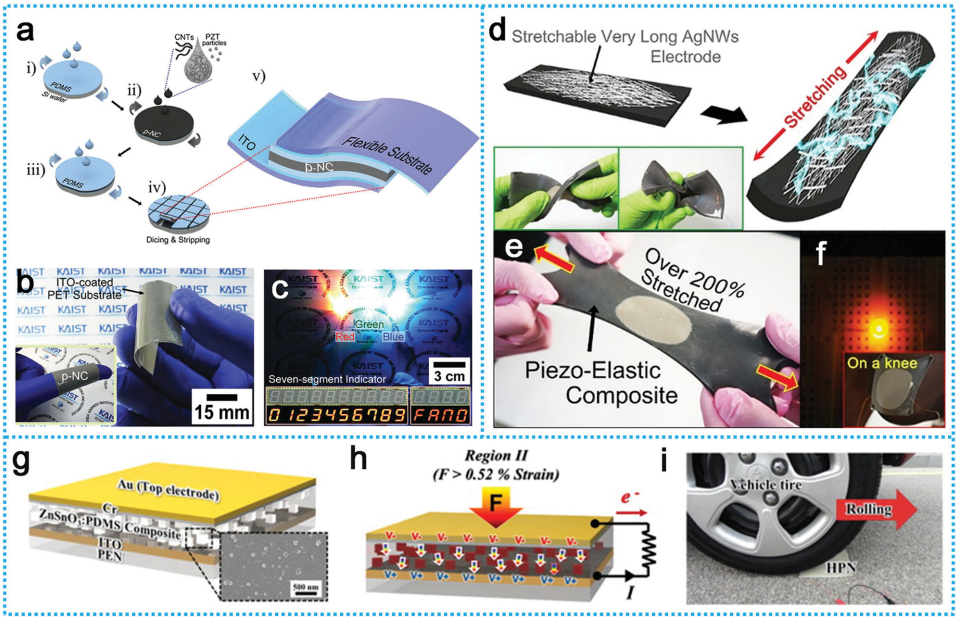

Figure 10. a–c) Fabrication and feature presentation of flexible composite NG device with PZT particles and MWCNTs. Reproduced with permission.[89] Copyright 2013, Wiley-VCH. d) Structure of the $ZnSnO_3$-PDMS composite-based flexible hybrid NG and power generation under a rolling tire. Reproduced with permission.[90] Copyright 2014, Wiley-VCH. e–g) A hyper-stretchable and deformable elastic-composite NG consisting of well-dispersed PMN-PT particles and MWCNTs with a silicone-rubber matrix. Reproduced with permission.[97] Copyright 2015, Wiley-VCH.

twisting, folding, and crumpling, or a stretching motion, the composite-based nanogenerator could directly generate the power output while maintaining mechanical and electrical robustness. The device was sewn onto the knee of a nylon stocking to demonstrate the feasibility for driving commercial electronics and integrating on clothes as wearable electronics.

3. Flexible Triboelectric Nanogenerator

Triboelectrification is conventionally known since the ancient Greek era and usually taken as a negative effect. However, tactfully based on a conjunction of triboelectrification and electrostatic induction, triboelectric nanogenerator (TENG) is invented recently, which could convert mechanical energy into electricity. Considering triboelectrification ubiquitously exists in the surrounding environment and for any most common materials used every day, TENGs could be inherently flexible and meanwhile serve as an energy source for our daily increasing portable or implantable electronic device, or as one of self-powered environmental sensors in the future internet of things.

3.1. Invention and Working Principle

In 2012, a simple, cost-effective and all-polymer based flexible triboelectric nanogenerator (TENG) for harvesting mechanical energy, through a conjunction of triboelectrification and electrostatic induction, was demonstrated.[98] The TENG consists of two polymer films, that have different electron-attracting abilities, with metal films deposited on their back sides (**Figure 11**a). When the two films contact, friction happens, owing to the natural nanoscale surface roughness, which leads to equal amount but opposite signs of charges generate at the two films' surfaces. Thus, an electric potential is formed at the interface region. As the two films contact and separate, the alternative potential will drive electrons in the external load to flow back and forth. Such a typical flexible polymer TENG yields an output voltage of up to 3.3 V and a power density of 10.4 μW cm^{-3}.

This mode is vertical contact-separation mode of TENG. A detailed working principle is shown in Figure 11b. When the TENG is pressed, the two tribo-materials contact. According to previous works,[14,99] due to their different electron-attracting abilities, electrons could be transferred from one material to another, thus there will be net negative charges on the surface of the layer with a strong electron attracting ability and net positive charges on the other (Figure 11b (II)). As the two tribo-materials separate, the tribo-charges in the interfacial regions are separated, which will induce an electrical potential in the interfacial region, therefore electrons in the attached induction electrodes will be driven to flow from one side to another (forming a current flow, Figure 11b (III)). In this process, electrons keep flowing until the TENG is fully released, which is represented by Figure 11b (V). At this moment, both

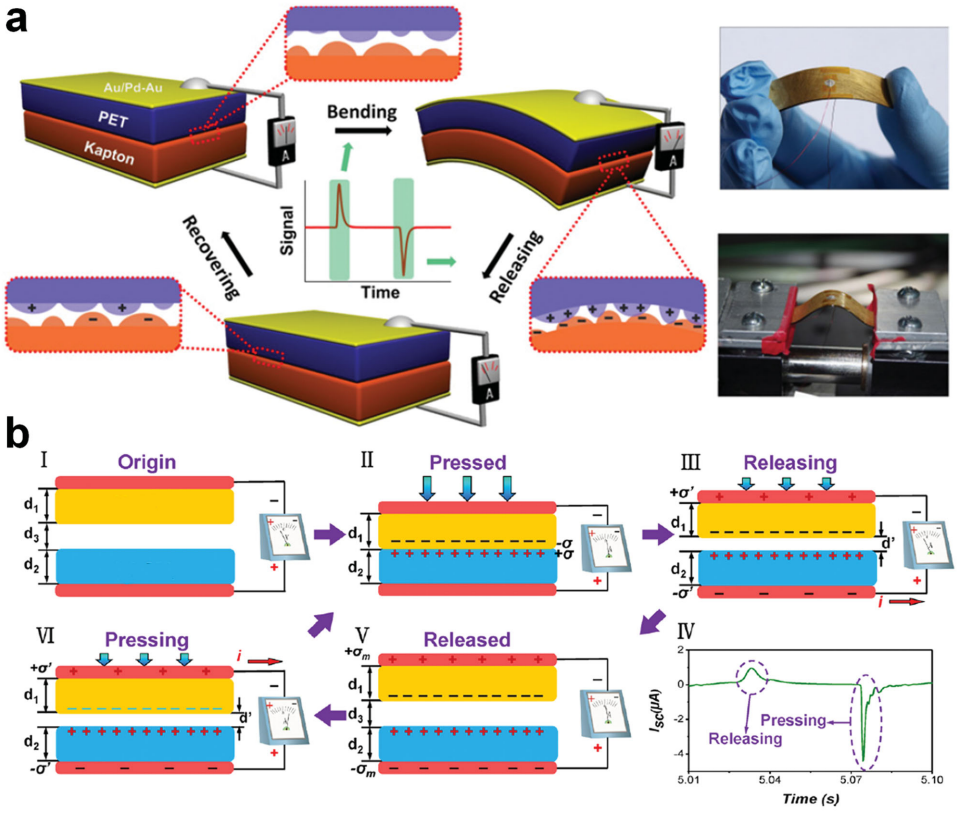

Figure 11. Invention and working principle of the flexible triboelectric nanogenerator. a) The construction and photography images of the first flexible triboelectric nanogenerator. Reproduced with permission.[98] Copyright 2012, Elsevier. b) Working principle of the TENG. Reproduced with permission.[99] Copyright 2012, American Chemical Society.

Adv. Mater. **2016**,
DOI: 10.1002/adma.201504299

the induced potential difference and the amount of transferred charges reach the maximum values. As the two tribo-materials approach, the potential difference will drop and the electrons will flow back (Figure 11b (VI)). Thus, the entire process will generate an alternative current (AC) pulse output.

3.2. Structural Designs

3.2.1. Arch and Stacking Structures

After the first TENG was reported in 2012, a variety of different designs have been proposed,[19,100–104] even new working modes have been developed.[15,105,106] Amongst them, the arch-shaped structure is one of the most classical designs, due to its high performance, simple fabrication, universal feasibility and durability.[107–111] As shown in **Figure 12**a, this device utilizes the contact electrification between a polymer film and a metal foil, with an arch-shaped gap between. The detailed fabrication method can be found in the reference.[100] Its open-circuit voltage and short-circuit current reaches 230 V and 94 μA, respectively, and the energy conversion efficiency is in the range of 10–39%. It is further demonstrated to drive hundreds of light-emitting diodes and also charge the lithium ion battery to power a wireless sensing system, as well as a commercial mobile phone. This work demonstrates for the first time that the nanogenerator can drive personal mobile electronics.

Soon, various structures based on the arch shape are proposed. Figure 12b shows a spring structure that is based on stacked arch-shaped structures.[112] It consists of alternatively-stacked arch-shaped and anti-arch-shaped TENGs that are electrically connected in a parallel configuration. This type of TENG significantly enhances the device's output performance, with an output of 740 V and 184.6 μA, in which only two arch units are utilized. Another variation of the stacked arch-shaped structure is the zigzag structure.[113] With a 6-layered construction, the device outputs 656 μA.

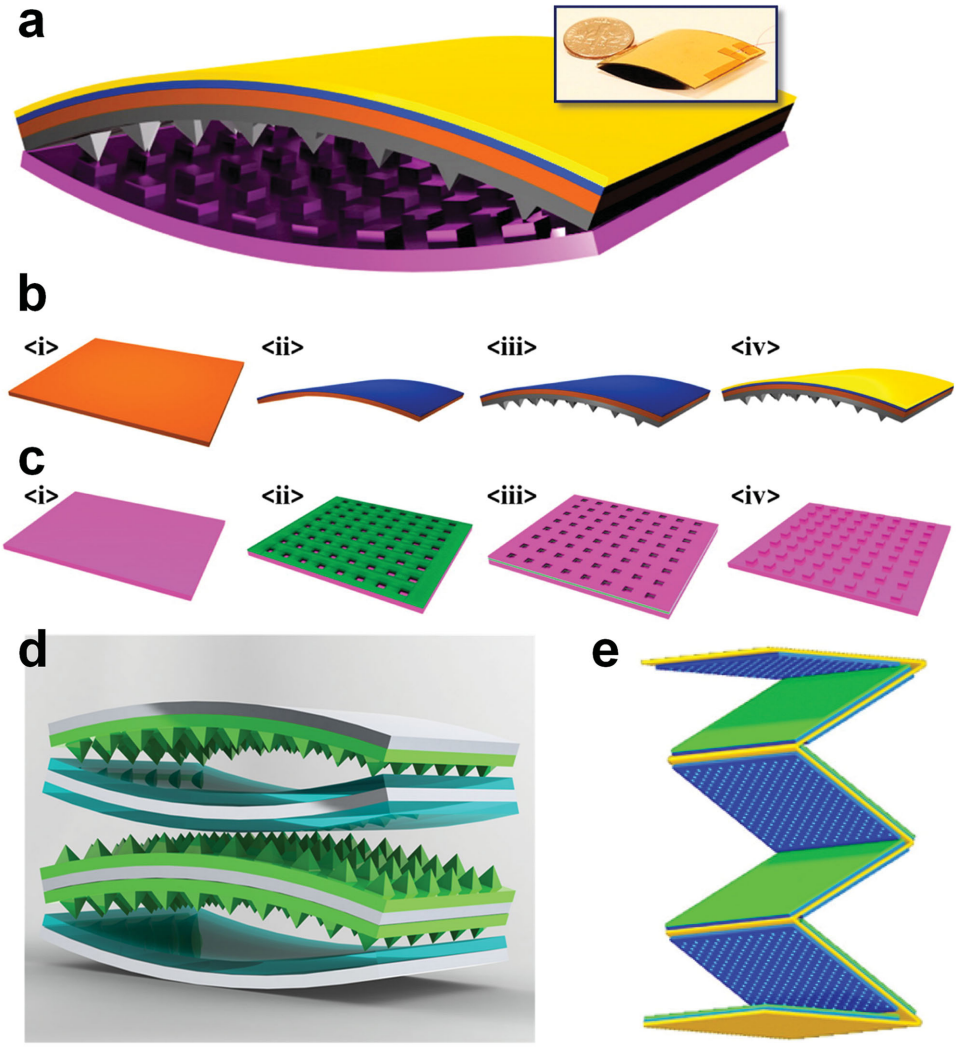

Figure 12. Structure evolution for the classic arch-shaped TENGs. a–c) Arch-shaped TENG and the fabrication process. Reproduced with permission.[100] Copyright 2012, American Chemical Society. d) Stacked arch-shaped TENGs. Reproduced with permission.[112] Copyright 2013, Elsevier. e) Zigzag TENGs. Reproduced with permission.[113] Copyright 2013, American Chemical Society.

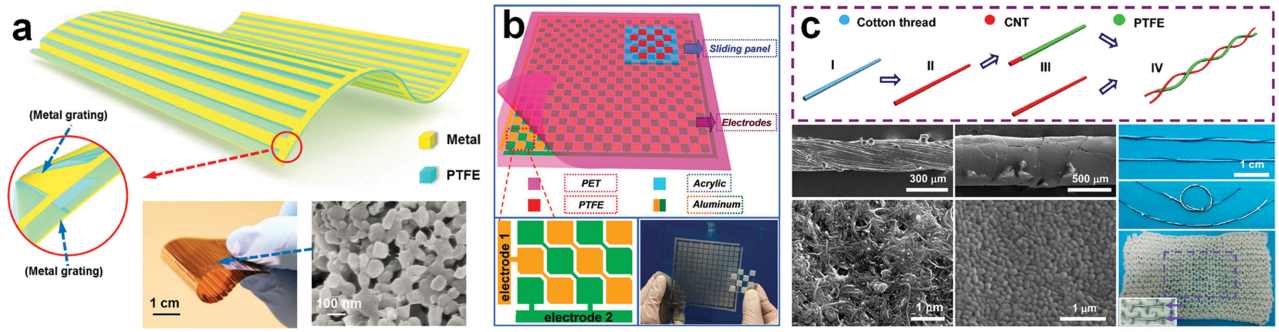

Figure 13. Alternative flexible structural designs. a) Micro-grating TENG with a high output performance. Reproduced with permission.[17] Copyright 2014, Wiley-VCH. b) Checker-like TENG. Reproduced with permission.[114] Copyright 2015, Wiley-VCH. c) Fiber-based TENG. Reproduced with permission.[115] Copyright 2014, American Chemical Society.

3.2.2. In-Plane Structures

In addition to the vertical contact-separation mode, the in-plane sliding mode is another option for the flexible TENGs. A thin-film-based micrograting triboelectric nanogenerator (MG-TENG) is displayed in **Figure 13**a.[17] It is made of complementary micro-sized arrays of linear grating, and can convert the relative sliding motion between two surfaces into electricity. Such a device with 60 cm^2 in area, 0.2 cm^3 in volume and 0.6 g in weight, is capable of delivering a peak current of 10 mA and a output power of 3 W with the conversion efficiency of ≈50%, when the sliding velocity is about 10 m s^{-1}. It can power regular electronics, such as light bulbs.

In order to convert translation kinetic energy in both x and y directions to electricity, Xi et al. developed a TENG based on checker-like interdigital electrodes with a sandwiched polyethylene terephthalate (PET) thin film (Figure 13b).[114] The performance of this TENG during different sliding directions is studied. It outputs a maximum power density of 1.9 W m^{-2} and a voltage of 210 V, in either x or y sliding direction. Furthermore, the author developed a mouse pad and sliding panel based on this TENG. It is found that the mouse operation energy could be harnessed to light up LEDs while the computer mouse operates an electronic game.

Unlike the above the two TENGs, fiber-based triboelectric generator (FB-TENG) is three-dimensional, and have the advantage of harvesting the energy from all directions, based on both vertical mode and in-plane mode.[115–117] Zhou et al. proposes a FB-TENG, fabricated through a facile, cost-effective method by using carbon nanotubes, a polytetrafluoroethylene (PTFE) aqueous suspension, and cotton threads.[115] This TENG can be worn around the arm or wrist, and are capable of converting living creatures' motions/vibration energy into electricity with a power density of ≈0.1 μW cm^{-2}. Additionally, it is fabricated as a power shirt, which could drive a wireless body temperature sensing system (Figure 13c).

3.3. Factors Determining the Output Performance

Since triboelectricfication is a surface charging effect, the surface morphology and friction materials will essentially determine the output of TENGs. This section will discuss about these factors.

3.3.1. Surface Morphology

To enlarge the friction area and further enhance the devices' output performance, researchers have implemented micro patterns, micro/nano dual-scale patterns and nano patterns onto the tribo-surfaces. **Figure 14**a compares the output of a typical TENG with four different PDMS surface types: plane, line, cube, and pyramid,[118] which are produced from the relative silicon mold. The testing results show that the increasing amplitude of the output follows the order of film < line < cube < pyramid. Specifically, when the TENG is triggered at a frequency of 0.33 Hz, with a strain of 0.13%, its maximum output voltage and current for the pyramid-featured device are 18 V and 0.7 μA respectively, almost four times as high as that of the plane one.

Afterwards, Zhang et al. investigated micro/nano dual-scale patterns' influence on the TENG's output (Figure 14b).[119] It is believed that the dual-scale patterns could significantly increase the effective roughness compared to the plane film, and thus enhance the TENG's performance. Experiments demonstrate that the micro/nano dual-scale PDMS film with pyramid arrays enlarged the output voltage and current by 100% and 157%, respectively, than those of flat PDMS film.

Lee et al. utilized the block copolymer (BCP) technology to further bring together a broad range and practical method to obtain densely arranged nanoscale patterns including dots, lines, holes, and rings, as shown in Figure 14c.[120] Testing results show that the flat-surface TENG generated open-circuit voltages and short-circuit current densities of up to ≈63 V and ≈1.1 mA m^{-2}, respectively, when the vertically compressive force of 50 N was applied. In clear contrast, the voltage and current density of the BCP-patterned TENGs with nanodots, nanogrates, and nanomeshes have increased from ≈95 V and ≈1.8 mA m^{-2}, to ≈110 V and ≈2.3 mA m^{-2}, and to ≈130 V and ≈2.8 mA m^{-2}, respectively.

3.3.2. Materials

The material properties, such as the electron affinity, work function, friction, and so on, also play important roles in TENGs' output performance. A vast amount of advanced materials have been investigated, including graphene,[121–123] carbon nanotube,[111,124] nano-Ag ink,[125] etc.

Adv. Mater. **2016**,
DOI: 10.1002/adma.201504299

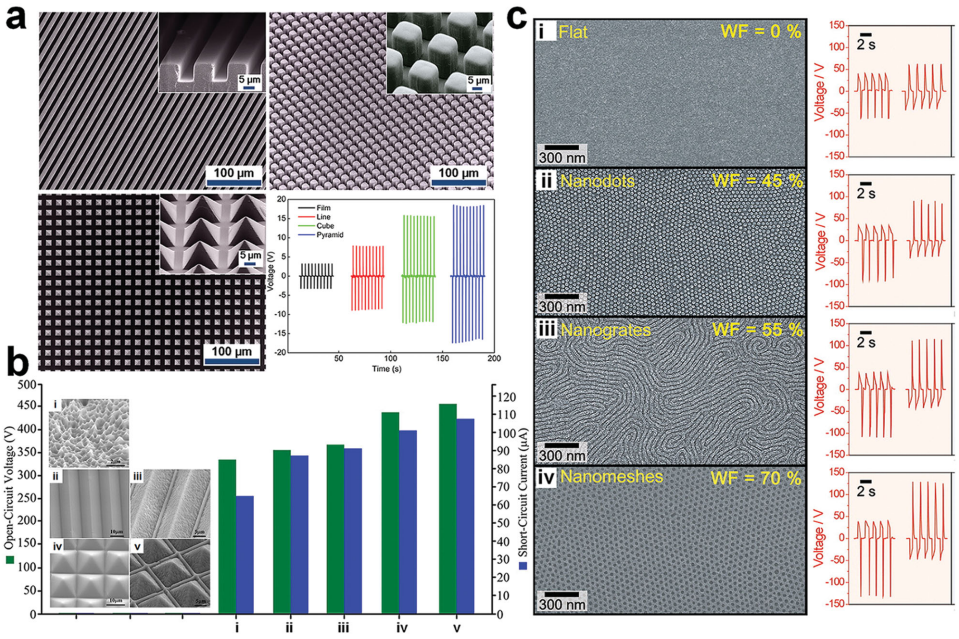

Figure 14. Influence of surface morphology on the TENG's output performance. a) Micro patterns. Reproduced with permission.[118] Copyright 2012, American Chemical Society. (b) Micro/nano dual-scale patterns. Reproduced with permission.[119] Copyright 2013, Elsevier. c) Nanopatterns. Reproduced with permission.[120] Copyright 2014, American Chemical Society.

Theoretical investigations on the electrostatic behavior of graphene are reported,[126,127] and it is found that graphene can store the electric charge, which suggests its applications in TENGs. And its nano-scale roughness and friction might increase the surface charges. Therefore, Kim et al. studied the graphene-based TENG (G-TENG).[121] As shown in **Figure 15**a, four kinds of G-TENGs are designed, including one-layer (1L), two-layer (2L), three-layer (3L), and four-layer (4L) graphene devices, by using a layer by layer transfer technique. It is found that the output voltage and current for the 1L-, 2L-, 3L-, and 4L-GTNGs decrease with the increasing number of graphene layers, which are 5.0, 3.0, 2.0, and 1.2 V for the voltage, and 500, 250, 160, and 100 nA cm^{-2} for the current density. The observed results are explained in terms of work function and friction, which arises owing to different electronic interactions between randomly- and regularly- stacked graphene layers. Liu et al. currently investigated the roll-to-roll fabrication of the grapheme-based TENG.[122]

Due to that the carbon nanotube (CNT) film has high conductivity, stretchability, and triboelectric properties when contacting the PDMS, Bao et al. developed the CNT-based TENG (Figure 15b).[124] Such a device could deliver an output voltage and current in the range of tens of volts and tenths to several μA cm^{-2}. Afterwards, it is fabricated as a self-powered pressure sensor, which shows a high pressure sensitivity (maximum value of 1.5 kPa^{-1} when the pressure under 1 kPa).

Recently, Kim et al. reported a novel sponge structure-based TENG. This device exhibits a stable output under a

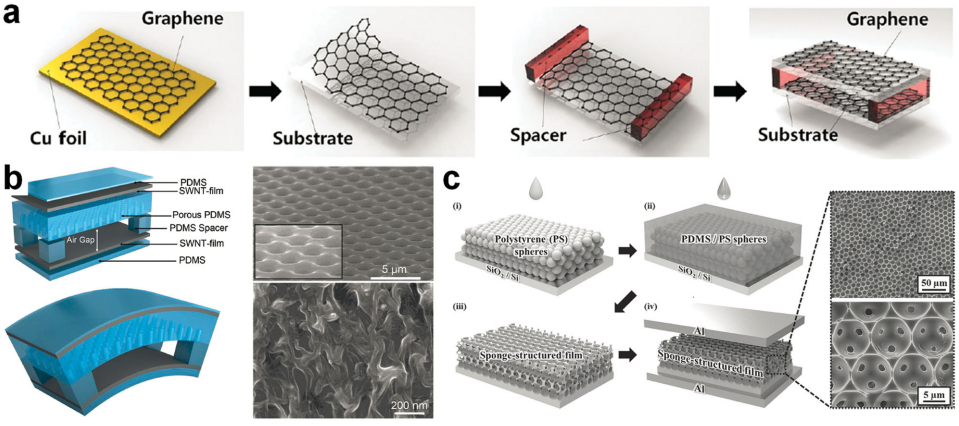

Figure 15. Influence of the material selection on the TENG's output performance. a) Graphene-based TENG. Reproduced with permission.[121] Copyright 2014, Wiley-VCH. b) CNT-based TENG. Reproduced with permission.[124] Copyright 2014, Wiley-VCH. c) Sponge-based TENG. Reproduced with permission.[128] Copyright 2014, Wiley-VCH.

wide range of humid conditions.[128] It consists of a highly compressible inverse opal-structured PDMS film and a Al film (Figure 15c). As for the fabrication, the authors first deposited a polystyrene (PS) microspheres layer on a SiO_2/Si substrate. Then, they deposited PDMS around the microspheres, etched the polystyrene spheres, and finally transferred the sponge layer on to the Al electrode. The obtained sponge layer is found to possess a Young's modulus that is 30% smaller and much more flexible compared to the original PDMS material. Therefore, under the same mechanical stress, the compressed sponge layer is thinner than the equivalent PDMS film, enabling the capacitance of the compressed sponge layer to increase due to a higher e/d ratio. Moreover, the sponge layer remarkably increases the contact area. Testing results shows that the output voltage and current of the sponge-structure TENG increases up to 130 V and 0.10 mA cm^{-2}, which means a 10-fold power enhancement, compared with the flat PDMS TENG.

As for other material choices, paper has been popular,[38,129,130] due to that it is cheap, lightweight, disposable, environmentally friendly, and the paper-based functional electronic devices would have wide applications in sensors and transistors. In addition, chemical modification and surface charging for the friction material, e.g., via the fluorocarbon plasma treatment,[131] or ionized-air injection[132] have also been proposed by researchers.

3.4. Integration and Fabrication

The rapid development shows the flexible TENGs' suitability for the practical applications, but will require research on the integration of the TENG with electronic devices and a more efficient industrial fabrication. This proceeding section will briefly describe the current updates on these.

Figure 16a presents a prototype of a flexible self-charging power unit (SCPU). It integrates a TENG-based energy harvester with a lithium-ion-battery (LIB)-based energy storage.[133] It can drive an external load and provides a constant voltage derived from the battery's intrinsic electrode potentials. Measurements show that the SCPU can supply a constant voltage with a current of 2 μA for 40 h, and it is able to continuously drive a UV sensor. In addition, Pu et al. further designed a wearable power unit, by integrating a textile TENG-cloth and a flexible LIB belt (Figure 16b).[134] It is demonstrated that after charging by the TENG-cloth for three cycles, the LIB belt powered a heartbeat meter strap to remotely communicate with a smart phone, indicating the viability of the whole wearable smart electronics. These researches impact the traditional trends of battery research and advances the development of portable and wearable self-powered systems.[135–138] In terms of industrial fabrication, Meng et al. introduces a well-known method, flexible printed circuit (FPC) board technology, making the fabrication procedure efficient and cost-effective.[139] A 10 friction pairs with a zigzag structure was fabricated simply by this technology (Figure 16c), and delivered a voltage and current density of 620 V and 45.1 μA cm^{-2}. Most notably, the FPC technology yields a simple procedure to integrate electronic components with the TENG to form a self-powered system.[140,141]

3.5. Applications of the Flexible TENG

Because of its simple, cost-effective, and industrially available advantages, a vast quantity of researchers have been

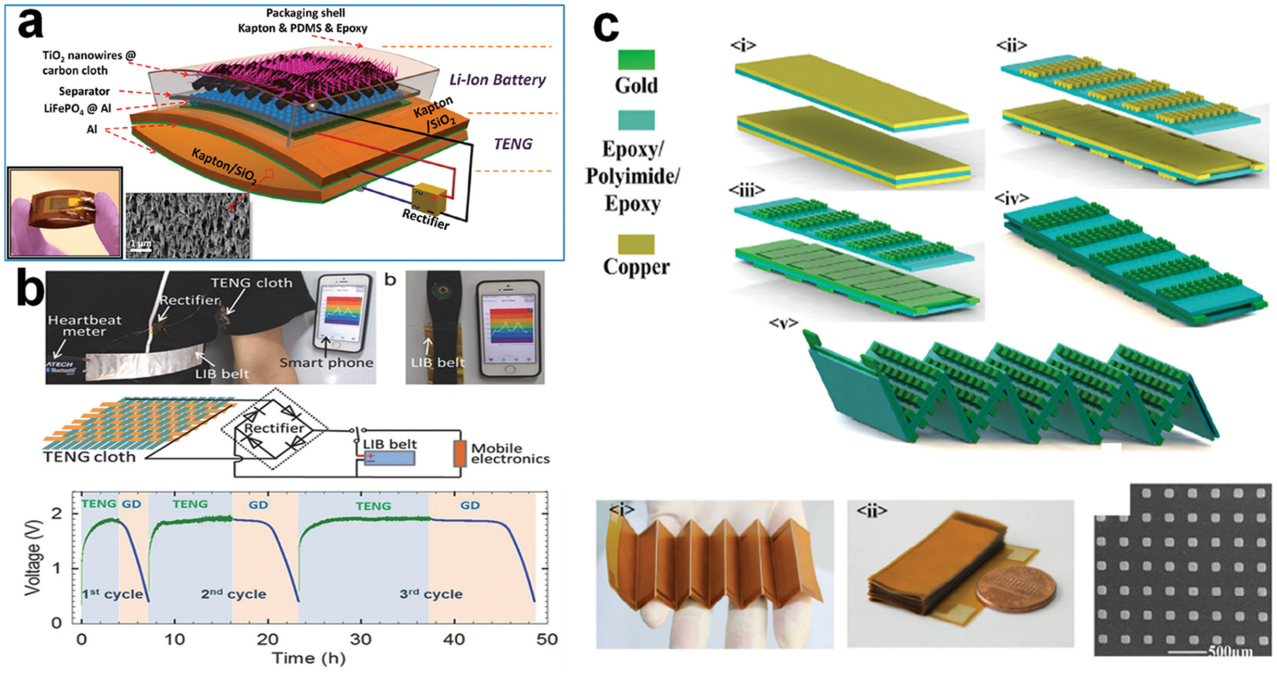

Figure 16. Miscellaneous works on flexible TENGs. a,b) Flexible self-charging power units. a) Reproduced with permission.[133] Copyright 2013, American Chemical Society. b) Reproduced with permission.[134] Copyright 2015, Wiley-VCH. c) PCB fabrication method for TENG. Reproduced with permission. [139] Copyright 2013, Elsevier.

Adv. Mater. 2016,
DOI: 10.1002/adma.201504299

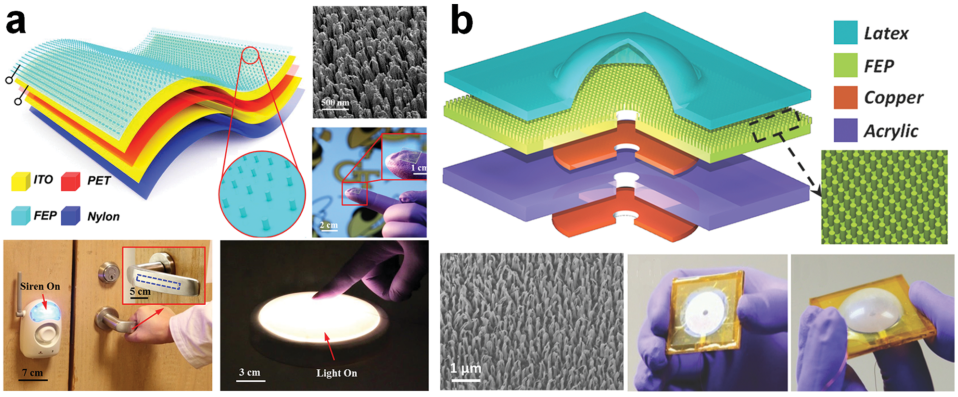

Figure 17. a) Self-Powered, ultrasensitive, flexible tactile sensors. Reproduced with permission.[37] Copyright 2014, American Chemical Society. b) Membrane-based self-powered sensors for pressure change detection. Reproduced with permission.[143] Copyright 2014, Wiley-VCH.

concerned with the TENG's practical applications. The applications of TENG in energy and sensors has been comprehensively reviewed previously.[14,15,19,106,142] In this section, we present a few examples regarding the applications of flexible TENGs to give a highlights. More details can refer to the review articles.

Since the vertical contact-separation mode is commonly used for the flexible TENG, the devices' output performance directly depends on magnitude/frequency of the external mechanical stimuli. In this regard, the most straightforward application for the flexible TENG could be the mechanical stimuli monitoring, such as pressure sensing.[37,103,118,143,144]

Figure 17a shows a self-powered tactile sensing system based on the TENG.[37] It could response to the contact electrification caused by external physical trigger, and generate a voltage signal without using any external power supply. The TENG sensor has polymer nanowires as the contact surface, and shows a high pressure sensitivity of 44 mV Pa^{-1} (0.09% Pa^{-1}). And when it works in a low-pressure region (<0.15 kPa), a maximum sensitivity of 1.1 V Pa^{-1} (2.3% Pa^{-1}) is obtained. In addition, the authors integrated it with a signal-processing circuit, and developed a tactile sensing system. As shown in Figure 17b, Bai et al. proposed another TENG sensor targeting for pressure change detection.[143] It is found that the sensor exhibits high resolutions of 0.34 Pa and 0.16 Pa, when the air pressure increases and decreases, respectively, in a small region away from the ambient atmosphere pressure. Similarly, by integrating the TENG sensor with a signal processing unit, the authors demonstrated applications of the device in sensing footsteps, respirations, and heartbeat. The above works could encourage TENGs' diverse applications, explicitly indicating automatic control, surveillance, remote operation, and security systems.

Besides pressure detecting, flexible TENGs could be inherently suitable to serve as self-powered touching pads. **Figure 18**a presents a human skin based TENG.[145] It utilizes the triboelectrification between the human skin and the PDMS film with a micropyramid-patterned surface. The testing results show the device could deliver an open-circuit voltage up to 1000 V, a current density of 8 mA m^{-2}, and a power density of 500 mW m^{-2} when the external load is 100 MΩ. Furthermore, the author utilized the TENG to design an addressed matrix for tracking the location of human touch, where the detection sensitivity is about 0.29 V kPa^{-1}.

Later, Chen et al. further developed an intelligent and self-powered keyboard as a safeguard against unauthorized access to computers, also based on TENGs (Figure 18b).[146] This

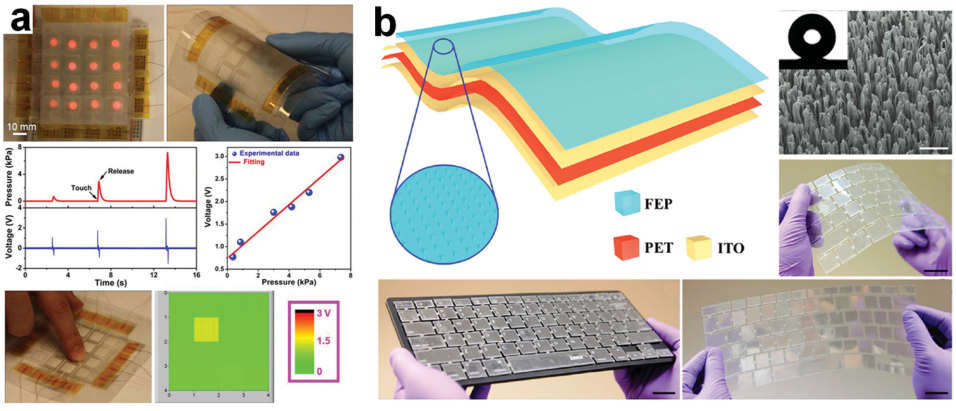

Figure 18. a) Human-skin-based active touching pads. Reproduced with permission.[145] Copyright 2013, American Chemical Society. b) Personalized keyboard for self-powered human machine interfacing. Reproduced with permission.[146] Copyright 2015, American Chemical Society.

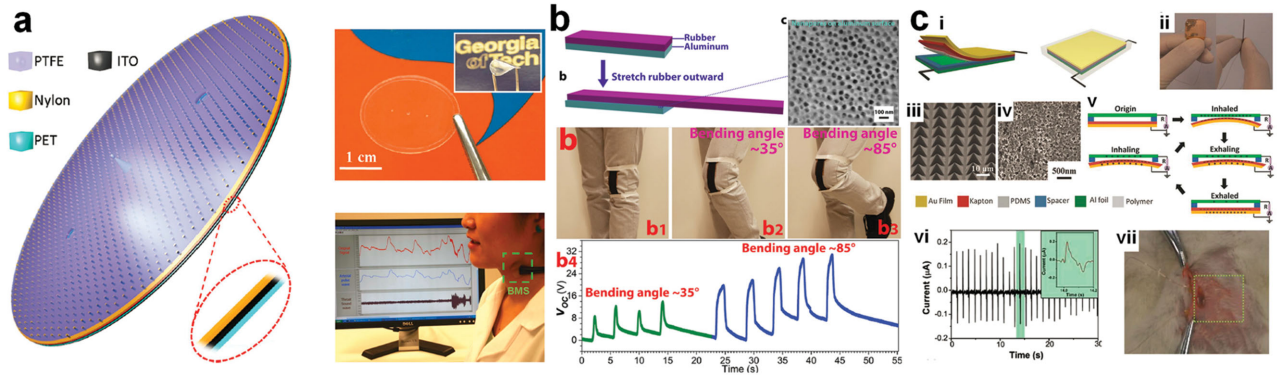

Figure 19. a) Self-powered cardiovascular system characterization and throat-attached anti-interference voice recognition. Reproduced with permission.[147] Copyright 2015, Wiley-VCH. b) Self-powered body motion sensors. Reproduced with permission.[148] Copyright 2015, Wiley-VCH. c) In vivo powering of pacemaker by breathing-driven implanted triboelectric nanogenerator. Reproduced with permission.[149] Copyright 2014, Wiley-VCH.

intelligent keyboard (IKB) converts human typing kinetic energy into electricity that can be used for either touch-sensing or energy-harvesting purposes. As for the touch sensing, the IKB allows an identification of personality in data input using the dynamic electronic signals generated when striking keys. It is able to identify personal characteristics from different individuals, with a Equal Error Rate value of 1.34%. As for the power generating, the IKB can effectively harness the type motions, under a moderate typing speed of 350 characters per minute (CPM), to generate power and charge a commercial capacitor at a rate of 0.019 V s^{-1}, which provides a feasible means of utilizing the wasted typing energy.

Due to the wearable and lightweight features, the TENG has promising application potential in the medical field. Yang et al. developed a self-powered bionic membrane sensor (BMS), based on the TENG technology, with a human eardrum-like structure (**Figure 19**a).[147] It shows a sensitivity of 51 mV Pa^{-1} and its response time is less than 6 ms. The BMS is then demonstrated to measure the dynamic pressure patterns of human cardiovascular system, and be able to serve as an anti-interference throat microphone, which could be used for recovering the human throat voice in an extremely noisy environment.

Figure 19b shows a self-powered body motion sensor. It consists of a layer of elastic rubber and an aluminum film serving as the electrode.[148] By stretching and releasing, the tribocharge distribution/density on the rubber surface will change, so that an alternating current will occur between the aluminum electrode and the ground. The device could be set over the knee joint. When humans bending or releasing the knee, the device generates output voltage signals, corresponding to the knee's bending angle. Therefore, the knee's bending rate can be monitored by this device.

As a power source, the flexible TENG is integrated with a pace maker and implanted in the living creature by Li et al.[149] The authors demonstrated that the breathing generated energy could be directly harnessed by the TENG to power a prototype pacemaker (Figure 19c). Similarly, a portable and implantable self-powered laser cure system is also demonstrated.[150] These works bring a bright future for the lifetime wearable or implantable self-powered medical/curing devices.[151]

4. Flexible Hybrid Nanogenerators

Our surrounding environment has an abundance of wasted energy in various forms, such as mechanical, thermal, optical, chemical, biological. After the first hybrid cell was demonstrated in 2009,[152] innovative approaches to hybrid energy harvesting techniques have been extensively developed in recent years because of the potential to harvest multiple types of energy sources in an effective manner that can be complimentarily utilized regardless of the availability of one or all of the sources.[153,154] In the following part, we will briefly introduce the lasted developments in flexible and stretchable hybrid NGs for simultaneously harvesting multi-type energy sources.

Flexible mechanical energy harvesters have been designed and fabricated based on principles of piezoelectric and triboelectric effect, as well as their cumulative effect. Han et al. designed an *r*-shaped hybrid nanogenerator using PVDF film, nanostructured Al electrodes, and micro-patterned PDMS film, combining the piezoelectric NG and the triboelectric NG to enhance the output performance (**Figure 20**a).[155] The output voltage, current density, and volume power density of the piezoelectric NG reach up to 52.8 V, 20.75 μA cm^{-2}, and 10.95 mW cm^{-3}, respectively; for the triboelectric NG, 240 V, 3.40 μA cm^{-2}, and 2.04 mW cm^{-3}, respectively. Through one cycle of electricity generation, 10 LEDS are instantaneously operated and a LCD display can continuously work for more than 15 s. By implementation of an identical structure, Jung et al. demonstrated a hybrid NG that integrates a PENG and a TENG by using PVDF film, metal electrodes, and PTFE film (Figure 20b).[156] The device combines high piezoelectric output current and triboelectric output voltage that can be powered by using both piezoelectric and triboelectric effects simultaneously in one operating cycle (Figure 20c). This hybrid generator produces a peak output voltage of 370 V, a current density of 12 μA cm^{-2}, and an average power density of 4.44 mW cm^{-2}, which can successfully light up 600 LED bulbs by the force of fingers (≈0.2 N). Li et al demonstrated a 3D fiber-Based hybrid nanogenerator composed of TENG and PENG to collect the mechanical energy in the environment.[116] The hybrid NG allows for the feasibility of enhancing the output power of NGs to meet different application benchmarks.

Adv. Mater. **2016**,
DOI: 10.1002/adma.201504299

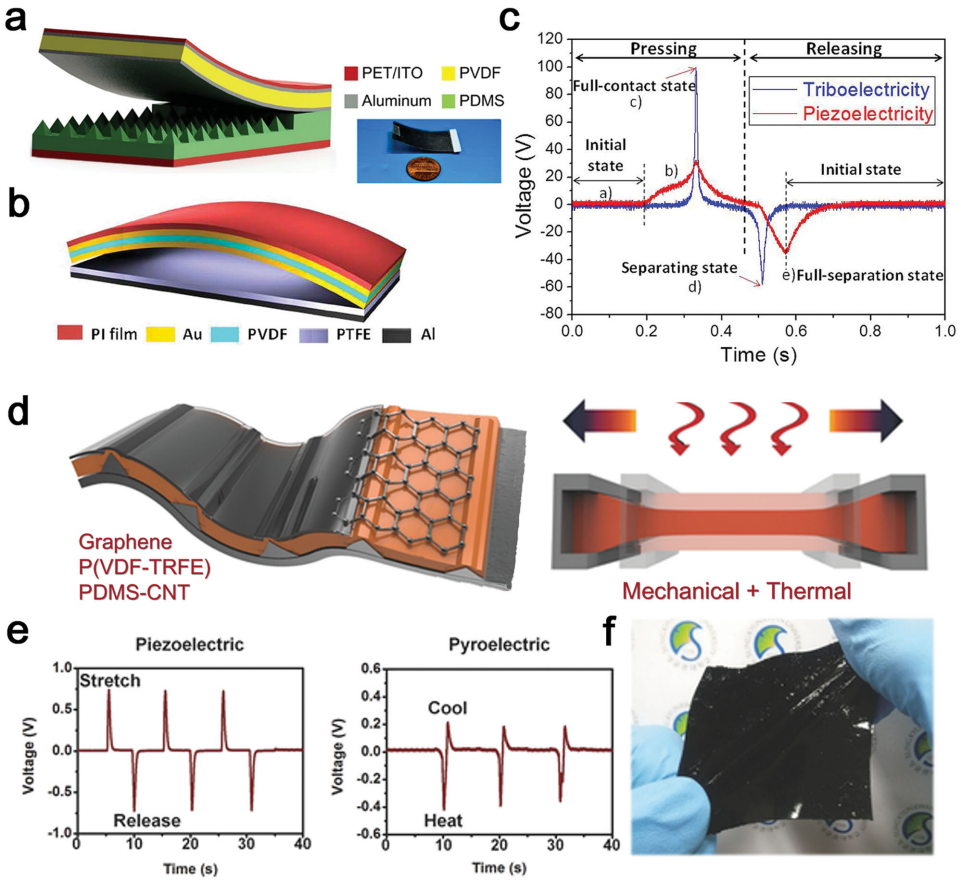

Figure 20. a–c) Schematic view of two similar structures of piezotriboelectric hybrid NGs with enhanced output voltages. a) Reproduced with permission.[155] Copyright 2013, American Chemical Society. b-c) Reproduced with permission.[156] Copyright 2015, Nature Publishing Group. d–f) A highly stretchable piezoelectric–pyroelectric hybrid NG for harvesting mechanical and thermal energy from a single device under various modes of applied strain and a present thermal gradient. Reproduced with permission.[157] Copyright 2014, Wiley-VCH

Lee et al. fabricated a highly stretchable, hybrid energy-scavenging NG using a micropatterned piezoelectric P(VDF-TrFE) film, PDMS-CNT composite, and graphene.[157] As shown in Figure 20d–f, the NG device with PDMS-CNT is fully stretchable and flexible. PDMS-CNT serves as the bottom electrode while graphene is the top electrode because of its high thermal conductivity. The hybrid NG can synchronously generate a piezoelectric output voltage under stretching, releasing conditions and a pyroelectric output voltage under thermal gradients i.e., heating and cooling in proximity to the device. It was observed that the line-based micro-pattern PDMS-CNT composite greatly enhances the stretchability, mechanical durability and robustness of the piezoelectric film. Such a stretchable and flexible hybrid energy harvester would have high applicability in many fields, e.g., wireless sensors, medical diagnostics, and self-powered biomedical system.

Solar cell is one kind of popular renewable energy with a large economic global market. For environmental conditions without sufficient sunlight, it requires a supplementary energy harvesting method to avoid the shortage of energy and to provide continuous and stable electrical output for the sensor devices. Recently, Choi et al. presented a flexible hybrid NG that simultaneously converts mechanical and solar energy into electrical energy using piezoelectric ZnO in conjunction with an organic solar cell design.[158] To achieve full flexible devices, an polymer substrate coated with an indium tin oxide (ITO) layer was selected as a cathode in terms of a solar cell, followed by a ZnO nanowire film, a photoactive layer, molybdenum oxide (MoO_x) layer, and a metal anode (**Figure 21**a). In terms of its solar cell performance, the power conversion efficiency (PCE) of average 1.5% was obtained with an open circuit voltage of 0.55 V and a short circuit current density of 9.2 mA cm^{-2} in a standard AM 1.5 G illumination condition. The piezoelectric output voltage was up to 150 mV and the output current was about hundreds of nA. Under a controlled mechanical straining process, the device show enhanced performance in both solar and mechanical energies synergistically (Figure 21b).

To simultaneously scavenge solar, mechanical and thermal energy, Yang et al. demonstrate a flexible hybrid cell (HC) that consists of a pyroelectric NG, a piezoelectric NG, and a solar cell.[159] As illustrated in Figure 21c, the bottom piezoelectric and pyroelectric NG consists of two Ag electrodes and a polarized PVDF film. The top solar cell consists of an Ag electrode, a ZnO nanowire array-poly(3-hexylthiophene) (P3HT) hetero-junction deposited on an ITO film electrode. Under AM 1.5 illumination with 100 mW cm^{-2} light intensity, the solar cell device produces an output voltage of 0.41 V and an output current density of 31 μA cm^{-2}. The pyroelectric NG

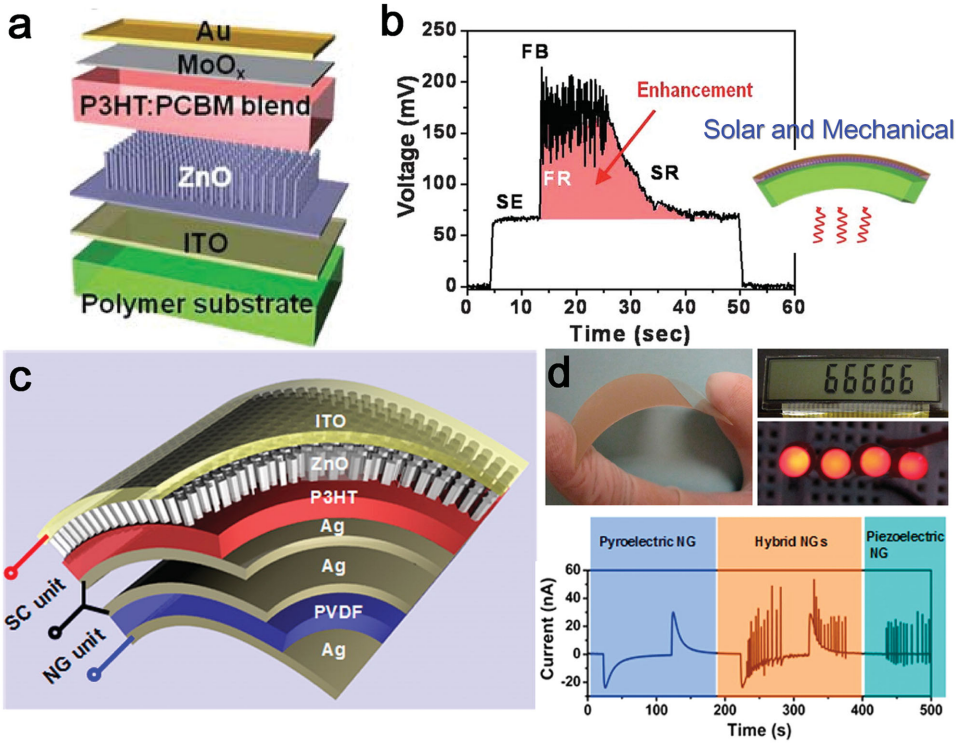

Figure 21. a) Schematic illustration of the structure of a hybrid cell consisting of a solar cell and a NG. b) Output voltage measured by controlling straining processes under solar illumination. a,b) Reproduced with permission.[158] Copyright 2011, Royal Society of Chemistry. c,d) A flexible hybrid energy cell can be implemented for simultaneously harvesting thermal, mechanical, and solar energy. Reproduced with permission.[159] Copyright 2013, American Chemical Society.

can generate an output voltage of ≈3 V and an output current of ≈30 nA when the temperature shifts from 295 to 314 K, or vice versa. For the piezoelectric NG under a periodically applied force, the output voltage and current were ≈0.5 V and ≈20 nA, respectively. When both conditions of changing temperature and a periodic force were applied, the hybrid energy cell was capable of simultaneously delivering both types of energy. The energy produced by the hand-pressed HC device was capable of directly driving an LCD display. Moreover, the hybrid energy can also be stored in a Li-ion battery and used to drive four red LEDs in parallel connection (Figure 21d). These results indicate that the fabricated hybrid energy cell can simultaneously and individually scavenge mechanical, thermal, and solar energy.

5. Summary and Perspective

In this review, the recent progress of flexible piezoelectric nanogenerators and flexible triboelectric nanogenerators are systematically summarized. Since the first publication on the PENG in 2006 and the TENG in 2012, the output performance of NGs have been enhanced by several orders of magnitude. With substantial progress already being made, we anticipate significant advances in the near future, specifically from the coupling of highly efficient nanogenerators with flexible platforms. It could be expected that this technology will have a drastic impact that could possibly lead to a paradigm shift for applications in our daily lives.

Striving toward the development of flexible nanogenerators and its future applications, the following research aspects need to be considered and more work should be focused in order to address certain issues and constraints.

1. The development of more effective flexible devices for mechanical energy harvesting. The extended understanding of the mechanism of energy conversion and charge transfer will facilitate the optimization of the output performance of nanogenerators in order to achieve a higher energy conversion efficiency. In addition, the development of new generator modes is also attractive and important.
2. Improving the performance of flexible nanogenerators. Besides their output power, other performance metrics still need to be optimized and improved to meet the demands of practical applications, including adequate flexibility, stability and durability. For their industrial production, the devices must be cost-effective, a facile fabrication route, and is easy to scale-up and integrate. New materials and new technologies would facilitate the accomplishment of this task.
3. Integration of flexible power sources with other electronic devices to fabricate completely self-powered flexible systems. The integration of flexible nanogenerators and flexible energy-storage devices, as well as a power management section is a feasible and the most effective alternative to drive mobile electronics, sensor networks, flexible electronics and wearable electronics. Hybrid energy cell harvesting multimode energy is also a promising and meaningful research direction.

Adv. Mater. **2016**,
DOI: 10.1002/adma.201504299

4. Paying more attention to flexible nanogenerators with novel structural designs to meet unconventional application requirements. In particular, flexible nanogenerators can be used for powering in vivo biomedical electronics (e.g., a self-powered cardiac pacemaker, implantable biosensor). Fiber-shaped nanogenerators can be combined with textile technologies to power wearable electronics. For macro-based applications, flexible TENGs prove to have a potential for harvesting ocean wave energy, namely blue energy harvesting.

Acknowledgements

F.R.F. and W.T. contributed equally to this work. Research was supported by the "thousands talents" program for pioneer researcher and his innovation team, China. We thank our group members and collaborators for their contributions to the work reviewed here.

Received: September 2, 2015
Revised: October 16, 2015
Published online:

[1] N. S. Lewis, *Science* **2007**, *315*, 798.
[2] M. S. Dresselhaus, I. L. Thomas, *Nature* **2001**, *414*, 332.
[3] Z. L. Wang, W. Wu, *Angew. Chem. Int. Ed.* **2012**, *51*, 11700.
[4] X. Chen, C. Li, M. Graetzel, R. Kostecki, S. S. Mao, *Chem. Soc. Rev.* **2012**, *41*, 7909.
[5] Z. L. Wang, *Sci. Am.* **2008**, *298*, 82.
[6] Z. L. Wang, J. H. Song, *Science* **2006**, *312*, 242.
[7] Z. L. Wang, *Nanogenerators for Self-Powered Devices and Systems*, Georgia Institute of Technology, Atlanta, GA, USA **2011**.
[8] Z. L. Wang, *Adv. Funct. Mater.* **2008**, *18*, 3553.
[9] Z. L. Wang, R. S. Yang, J. Zhou, Y. Qin, C. Xu, Y. F. Hu, S. Xu, *Mater. Sci. Eng. R* **2010**, *70*, 320.
[10] Y. Qi, M. C. McAlpine, *Energy Environ. Sci.* **2010**, *3*, 1275.
[11] K. Y. Lee, M. K. Gupta, S. W. Kim, *Nano Energy* **2015**, *14*, 139.
[12] Z. L. Wang, *Adv. Mater.* **2012**, *24*, 280.
[13] G. T. Hwang, M. Byun, C. K. Jeong, K. J. Lee, *Adv. Healthcare Mater.* **2015**, *4*, 646.
[14] Z. L. Wang, *ACS Nano* **2013**, *7*, 9533.
[15] Z. L. Wang, J. Chen, L. Lin, *Energy Environ. Sci.*, **2015**, *8*, 2250.
[16] X.-S. Zhang, M.-D. Han, B. Meng, H.-X. Zhang, *Nano Energy* **2015**, *11*, 304.
[17] G. Zhu, Y. S. Zhou, P. Bai, X. S. Meng, Q. S. Jing, J. Chen, Z. L. Wang, *Adv. Mater.* **2014**, *26*, 3788.
[18] W. Tang, T. Jiang, F. R. Fan, A. F. Yu, C. Zhang, X. Cao, Z. L. Wang, *Adv. Funct. Mater.* **2015**, *25*, 3718.
[19] Z. L. Wang, *Faraday Discuss.* **2014**, *176*, 447.
[20] G. Zhu, Y. J. Su, P. Bai, J. Chen, Q. S. Jing, W. Q. Yang, Z. L. Wang, *ACS Nano* **2014**, *8*, 6031.
[21] X. N. Wen, W. Q. Yang, Q. S. Jing, Z. L. Wang, *ACS Nano* **2014**, *8*, 7405.
[22] J. Chen, J. Yang, Z. L. Li, X. Fan, Y. L. Zi, Q. S. Jing, H. Y. Guo, Z. Wen, K. C. Pradel, S. M. Niu, Z. L. Wang, *ACS Nano* **2015**, *9*, 3324.
[23] Y. Sun, J. A. Rogers, *Adv. Mater.* **2007**, *19*, 1897.
[24] D.-H. Kim, N. Lu, R. Ma, Y.-S. Kim, R.-H. Kim, S. Wang, J. Wu, S. M. Won, H. Tao, A. Islam, K. J. Yu, T.-i. Kim, R. Chowdhury, M. Ying, L. Xu, M. Li, H.-J. Chung, H. Keum, M. McCormick, P. Liu, Y.-W. Zhang, F. G. Omenetto, Y. Huang, T. Coleman, J. A. Rogers, *Science* **2011**, *333*, 838.
[25] W. Zeng, L. Shu, Q. Li, S. Chen, F. Wang, X.-M. Tao, *Adv. Mater.* **2014**, *26*, 5310.
[26] Y. Chen, J. Au, P. Kazlas, A. Ritenour, H. Gates, M. McCreary, *Nature* **2003**, *423*, 136.
[27] M.-C. Choi, Y. Kim, C.-S. Ha, *Prog. Polym. Sci.* **2008**, *33*, 581.
[28] K. Takei, T. Takahashi, J. C. Ho, H. Ko, A. G. Gillies, P. W. Leu, R. S. Fearing, A. Javey, *Nat. Mater.* **2010**, *9*, 821.
[29] S. C. B. Mannsfeld, B. C. K. Tee, R. M. Stoltenberg, C. V. H. H. Chen, S. Barman, B. V. O. Muir, A. N. Sokolov, C. Reese, Z. Bao, *Nat. Mater.* **2010**, *9*, 859.
[30] C. Pan, H. Wu, C. Wang, B. Wang, L. Zhang, Z. Cheng, P. Hu, W. Pan, Z. Zhou, X. Yang, J. Zhu, *Adv. Mater.* **2008**, *20*, 1644.
[31] L. Nyholm, G. Nystrom, A. Mihranyan, M. Stromme, *Adv. Mater.* **2011**, *23*, 3751.
[32] X. Wang, X. Lu, B. Liu, D. Chen, Y. Tong, G. Shen, *Adv. Mater.* **2014**, *26*, 4763.
[33] K. Xie, B. Wei, *Adv. Mater.* **2014**, *26*, 3592.
[34] M. Koo, K.-I. Park, S. H. Lee, M. Suh, D. Y. Jeon, J. W. Choi, K. Kang, K. J. Lee, *Nano Lett.* **2012**, *12*, 4810.
[35] G. Zhou, F. Li, H.-M. Cheng, *Energy Environ. Sci.* **2014**, *7*, 1307.
[36] G. Zhu, R. Yang, S. Wang, Z. L. Wang, *Nano Lett.* **2010**, *10*, 3151.
[37] G. Zhu, W. Q. Yang, T. Zhang, Q. Jing, J. Chen, Y. S. Zhou, P. Bai, Z. L. Wang, *Nano Lett.* **2014**, *14*, 3208.
[38] X. Fan, J. Chen, J. Yang, P. Bai, Z. Li, Z. L. Wang, *ACS Nano* **2015**, *9*, 4236.
[39] K.-I. Park, M. Lee, Y. Liu, S. Moon, G.-T. Hwang, G. Zhu, J. E. Kim, S. O. Kim, D. K. Kim, Z. L. Wang, K. J. Lee, *Adv. Mater.* **2012**, *24*, 2999.
[40] G.-T. Hwang, H. Park, J.-H. Lee, S. Oh, K.-I. Park, M. Byun, H. Park, G. Ahn, C. K. Jeong, K. No, H. Kwon, S.-G. Lee, B. Joung, K. J. Lee, *Adv. Mater.* **2014**, *26*, 4880.
[41] Y. Qin, X. Wang, Z. L. Wang, *Nature* **2008**, *451*, 809.
[42] Z. Gao, J. Zhou, Y. Gu, P. Fei, Y. Hao, G. Bao, Z. L. Wang, *J. Appl. Phys.* **2009**, *105*, 113707.
[43] R. Yang, Y. Qin, L. Dai, Z. L. Wang, *Nat. Nanotechnol.* **2009**, *4*, 34.
[44] R. Yang, Y. Qin, C. Li, G. Zhu, Z. L. Wang, *Nano Lett.* **2009**, *9*, 1201.
[45] Z. Li, G. Zhu, R. Yang, A. C. Wang, Z. L. Wang, *Adv. Mater.* **2010**, *22*, 2534.
[46] S. Xu, Y. Qin, C. Xu, Y. Wei, R. Yang, Z. L. Wang, *Nat. Nanotechnol.* **2010**, *5*, 366.
[47] Y. Hu, Y. Zhang, C. Xu, G. Zhu, Z. L. Wang, *Nano Lett.* **2010**, *10*, 5025.
[48] L. E. Greene, M. Law, J. Goldberger, F. Kim, J. C. Johnson, Y. F. Zhang, R. J. Saykally, P. D. Yang, *Angew. Chem. Int. Ed.* **2003**, *42*, 3031.
[49] L. E. Greene, M. Law, D. H. Tan, M. Montano, J. Goldberger, G. Somorjai, P. D. Yang, *Nano Lett.* **2005**, *5*, 1231.
[50] M. Y. Choi, D. Choi, M. J. Jin, I. Kim, S. H. Kim, J. Y. Choi, S. Y. Lee, J. M. Kim, S. W. Kim, *Adv. Mater.* **2009**, *21*, 2185.
[51] D. Choi, M.-Y. Choi, H.-J. Shin, S.-M. Yoon, J.-S. Seo, J.-Y. Choi, S. Y. Lee, J. M. Kim, S.-W. Kim, *J. Phys. Chem. C* **2010**, *114*, 1379.
[52] E. B. Secor, S. Lim, H. Zhang, C. D. Frisbie, L. F. Francis, M. C. Hersam, *Adv. Mater.* **2014**, *26*, 4533.
[53] S. J. Kim, K. Choi, B. Lee, Y. Kim, B. H. Hong, *Annu. Rev. Mater. Res.* **2015**, *45*, 63.
[54] D. Choi, M.-Y. Choi, W. M. Choi, H.-J. Shin, H.-K. Park, J.-S. Seo, J. Park, S.-M. Yoon, S. J. Chae, Y. H. Lee, S.-W. Kim, J.-Y. Choi, S. Y. Lee, J. M. Kim, *Adv. Mater.* **2010**, *22*, 2187.
[55] Y. Hu, Y. Zhang, C. Xu, L. Lin, R. L. Snyder, Z. L. Wang, *Nano Lett.* **2011**, *11*, 2572.
[56] S. Lee, S.-H. Bae, L. Lin, Y. Yang, C. Park, S.-W. Kim, S. N. Cha, H. Kim, Y. J. Park, Z. L. Wang, *Adv. Funct. Mater.* **2013**, *23*, 2445.

[57] S. Lee, J. I. Hong, C. Xu, M. Lee, D. Kim, L. Lin, W. Hwang, Z. L. Wang, *Adv. Mater.* **2012**, *24*, 4398.
[58] M. Lee, C. Y. Chen, S. Wang, S. N. Cha, Y. J. Park, J. M. Kim, L. J. Chou, Z. L. Wang, *Adv. Mater.* **2012**, *24*, 1759.
[59] Z. T. Li, Z. L. Wang, *Adv. Mater.* **2011**, *23*, 84.
[60] Q. L. Liao, Z. Zhang, X. H. Zhang, M. Mohr, Y. Zhang, H. J. Fecht, *Nano Res.* **2014**, *7*, 917.
[61] N. Masghouni, J. Burton, M. K. Philen, M. Al-Haik, *Nanotechnology* **2015**, *26*, 095401.
[62] Y. Qiu, D. C. Yang, B. Yin, J. X. Lei, H. Q. Zhang, Z. Zhang, H. Chen, Y. P. Li, J. M. Bian, Y. H. Liu, Y. Zhao, L. Z. Hu, *RSC Adv.* **2015**, *5*, 5941.
[63] W. Zeng, X. M. Tao, S. Chen, S. M. Shang, H. L. W. Chan, S. H. Choy, *Energy Environ. Sci.* **2013**, *6*, 2631.
[64] C. L. Liu, W. G. Zhang, J. B. Sun, J. Wen, Q. Yang, H. X. Cuo, X. Z. Ma, M. Y. Zhang, *Appl. Surf. Sci.* **2014**, *322*, 95.
[65] S. Xu, B. J. Hansen, Z. L. Wang, *Nat. Commun.* **2010**, *1*, 93.
[66] J. Kwon, W. Seung, B. K. Sharma, S. W. Kim, J. H. Ahn, *Energy Environ. Sci.* **2012**, *5*, 8970.
[67] C. Dagdeviren, B. D. Yang, Y. W. Su, P. L. Tran, P. Joe, E. Anderson, J. Xia, V. Doraiswamy, B. Dehdashti, X. Feng, B. W. Lu, R. Poston, Z. Khalpey, R. Ghaffari, Y. G. Huang, M. J. Slepian, J. A. Rogers, *Proc. Natl. Acad. Sci. USA* **2014**, *111*, 1927.
[68] Y. Qi, N. T. Jafferis, K. Lyons, C. M. Lee, H. Ahmad, M. C. McAlpine, *Nano Lett.* **2010**, *10*, 524.
[69] Y. Qi, J. Kim, T. D. Nguyen, B. Lisko, P. K. Purohit, M. C. McAlpine, *Nano Lett.* **2011**, *11*, 1331.
[70] K. I. Park, J. H. Son, G. T. Hwang, C. K. Jeong, J. Ryu, M. Koo, I. Choi, S. H. Lee, M. Byun, Z. L. Wang, K. J. Lee, *Adv. Mater.* **2014**, *26*, 2514.
[71] X. Chen, S. Y. Xu, N. Yao, Y. Shi, *Nano Lett.* **2010**, *10*, 2133.
[72] L. Gu, N. Y. Cui, L. Cheng, Q. Xu, S. Bai, M. M. Yuan, W. W. Wu, J. M. Liu, Y. Zhao, F. Ma, Y. Qin, Z. L. Wang, *Nano Lett.* **2013**, *13*, 91.
[73] C. K. Jeong, K.-I. Park, J. H. Son, G. T. Hwang, S. H. Lee, D. Y. Park, H. E. Lee, H. K. Lee, M. Byun, K. J. Lee, *Energy Environ. Sci.* **2014**, *7*, 4035.
[74] C. E. Chang, V. H. Tran, J. B. Wang, Y. K. Fuh, L. W. Lin, *Nano Lett.* **2010**, *10*, 726.
[75] B. J. Hansen, Y. Liu, R. S. Yang, Z. L. Wang, *ACS Nano* **2010**, *4*, 3647.
[76] L. Persano, C. Dagdeviren, Y. W. Su, Y. H. Zhang, S. Girardo, D. Pisignano, Y. G. Huang, J. A. Rogers, *Nat. Commun.* **2013**, *4*, 1633.
[77] X. L. Chen, H. M. Tian, X. M. Li, J. Y. Shao, Y. C. Ding, N. L. An, Y. P. Zhou, *Nanoscale* **2015**, *7*, 11536.
[78] S. Cha, S. M. Kim, H. Kim, J. Ku, J. I. Sohn, Y. J. Park, B. G. Song, M. H. Jung, E. K. Lee, B. L. Choi, J. J. Park, Z. L. Wang, J. M. Kim, K. Kim, *Nano Lett.* **2011**, *11*, 5142.
[79] Y. C. Mao, P. Zhao, G. McConohy, H. Yang, Y. X. Tong, X. D. Wang, *Adv. Energy Mater.* **2014**, *4*, 1301624.
[80] R. M. Yu, L. Dong, C. F. Pan, S. M. Niu, H. F. Liu, W. Liu, S. Chua, D. Z. Chi, Z. L. Wang, *Adv. Mater.* **2012**, *24*, 3532.
[81] J. M. Wu, C. Xu, Y. Zhang, Z. L. Wang, *ACS Nano* **2012**, *6*, 4335.
[82] Q. H. Wang, K. Kalantar-Zadeh, A. Kis, J. N. Coleman, M. S. Strano, *Nat. Nanotechnol.* **2012**, *7*, 699.
[83] M. Chhowalla, H. S. Shin, G. Eda, L. J. Li, K. P. Loh, H. Zhang, *Nat. Chem.* **2013**, *5*, 263.
[84] W. Z. Wu, L. Wang, Y. L. Li, F. Zhang, L. Lin, S. M. Niu, D. Chenet, X. Zhang, Y. F. Hao, T. F. Heinz, J. Hone, Z. L. Wang, *Nature* **2014**, *514*, 470.
[85] H. Y. Zhu, Y. Wang, J. Xiao, M. Liu, S. M. Xiong, Z. J. Wong, Z. L. Ye, Y. Ye, X. B. Yin, X. Zhang, *Nat. Nanotechnol.* **2015**, *10*, 151.
[86] B. Y. Lee, J. X. Zhang, C. Zueger, W. J. Chung, S. Y. Yoo, E. Wang, J. Meyer, R. Ramesh, S. W. Lee, *Nat. Nanotechnol.* **2012**, *7*, 351.
[87] C. K. Jeong, I. Kim, K. I. Park, M. H. Oh, H. Paik, G. T. Hwang, K. No, Y. S. Nam, K. J. Lee, *ACS Nano* **2013**, *7*, 11016.
[88] K. I. Park, M. Lee, Y. Liu, S. Moon, G. T. Hwang, G. Zhu, J. E. Kim, S. O. Kim, D. K. Kim, Z. L. Wang, K. J. Lee, *Adv. Mater.* **2012**, *24*, 2999.
[89] K. I. Park, C. K. Jeong, J. Ryu, G. T. Hwang, K. J. Lee, *Adv. Energy Mater.* **2013**, *3*, 1539.
[90] K. Y. Lee, D. Kim, J.-H. Lee, T. Y. Kim, M. K. Gupta, S.-W. Kim, *Adv. Funct. Mater.* **2014**, *24*, 37.
[91] J. H. Jung, C. Y. Chen, B. K. Yun, N. Lee, Y. S. Zhou, W. Jo, L. J. Chou, Z. L. Wang, *Nanotechnology* **2012**, *23*, 375401.
[92] J. H. Jung, M. Lee, J. I. Hong, Y. Ding, C. Y. Chen, L. J. Chou, Z. L. Wang, *ACS Nano* **2011**, *5*, 10041.
[93] C. K. Jeong, K.-I. Park, J. Ryu, G.-T. Hwang, K. J. Lee, *Adv. Funct. Mater.* **2014**, *24*, 2620.
[94] K. Y. Lee, B. Kumar, J. S. Seo, K. H. Kim, J. I. Sohn, S. N. Cha, D. Choi, Z. L. Wang, S. W. Kim, *Nano Lett.* **2012**, *12*, 1959.
[95] S. Y. Chung, S. Kim, J. H. Lee, K. Kim, S. W. Kim, C. Y. Kang, S. J. Yoon, Y. S. Kim, *Adv. Mater.* **2012**, *24*, 6022.
[96] S. Y. Xu, Y. W. Yeh, G. Poirier, M. C. McAlpine, R. A. Register, N. Yao, *Nano Lett.* **2013**, *13*, 2393.
[97] C. K. Jeong, J. Lee, S. Han, J. Ryu, G.-T. Hwang, D. Y. Park, J. H. Park, S. S. Lee, M. Byun, S. H. Ko, K. J. Lee, *Adv. Mater.* **2015**, *27*, 2866.
[98] F.-R. Fan, Z.-Q. Tian, Z. L. Wang, *Nano Energy* **2012**, *1*, 328.
[99] G. Zhu, C. Pan, W. Guo, C.-Y. Chen, Y. Zhou, R. Yu, Z. L. Wang, *Nano Lett.* **2012**, *12*, 4960.
[100] S. Wang, L. Lin, Z. L. Wang, *Nano Lett.* **2012**, *12*, 6339.
[101] G. Zhu, Z.-H. Lin, Q. Jing, P. Bai, C. Pan, Y. Yang, Y. Zhou, Z. L. Wang, *Nano Lett.* **2013**, *13*, 847.
[102] G. Zhu, J. Chen, Y. Liu, P. Bai, Y. S. Zhou, Q. Jing, C. Pan, Z. L. Wang, *Nano Lett.* **2013**, *13*, 2282.
[103] L. Lin, S. Wang, Y. Xie, Q. Jing, S. Niu, Y. Hu, Z. L. Wang, *Nano Lett.* **2013**, *13*, 2916.
[104] Y. Yang, Y. S. Zhou, H. Zhang, Y. Liu, S. Lee, Z. L. Wang, *Adv. Mater.* **2013**, *25*, 6594.
[105] M. Ha, J. Park, Y. Lee, H. Ko, *ACS Nano* **2015**, *9*, 3421.
[106] S. Wang, L. Lin, Z. L. Wang, *Nano Energy* **2015**, *11*, 436.
[107] L. Lin, Y. Xie, S. Wang, W. Wu, S. Niu, X. Wen, Z. L. Wang, *ACS Nano* **2013**, *7*, 8266.
[108] J. Zhong, Q. Zhong, F. Fan, Y. Zhang, S. Wang, B. Hu, Z. L. Wang, J. Zhou, *Nano Energy* **2013**, *2*, 491.
[109] J. Chen, J. Yang, Z. Li, X. Fan, Y. Zi, Q. Jing, H. Guo, Z. Wen, K. C. Pradel, S. Niu, Z. L. Wang, *Acs Nano* **2015**, *9*, 3324.
[110] H. R. Zhu, W. Tang, C. Z. Gao, Y. Han, T. Li, X. Cao, Z. L. Wang, *Nano Energy* **2015**, *14*, 193.
[111] J. Luo, F. R. Fan, T. Zhou, W. Tang, F. Xue, Z. L. Wang, *Extreme Mech. Lett.* **2015**, *2*, 28.
[112] W. Tang, B. Meng, H. X. Zhang, *Nano Energy* **2013**, *2*, 1164.
[113] P. Bai, G. Zhu, Z.-H. Lin, Q. Jing, J. Chen, G. Zhang, J. Ma, Z. L. Wang, *ACS Nano* **2013**, *7*, 3713.
[114] H. Guo, Q. Leng, X. He, M. Wang, J. Chen, C. Hu, Y. Xi, *Adv. Energy Mater.* **2015**, *5*, 1400790.
[115] J. Zhong, Y. Zhang, Q. Zhong, Q. Hu, B. Hu, Z. L. Wang, J. Zhou, *ACS Nano* **2014**, *8*, 6273.
[116] X. Li, Z. Lin, G. Cheng, X. Wen, Y. Liu, S. Niu, *ACS Nano* **2014**, *8*, 10674.
[117] J. Wang, X. Li, Y. Zi, S. Wang, Z. Li, L. Zheng, F. Yi, S. Li, Z. L. Wang, *Adv. Mater.* **2015**, *27*, 4830.
[118] F. Fan, L. Lin, G. Zhu, W. Wu, R. Zhang, Z. Wang, *Nano Lett.* **2012**, *12*, 3109.
[119] X. Zhang, M. Han, R. Wang, F. Zhu, *Nano Lett.* **2013**, *13*, 1168.
[120] C. K. Jeong, K. M. Baek, S. Niu, T. W. Nam, Y. H. Hur, D. Y. Park, G. Hwang, M. Byun, Z. L. Wang, Y. S. Jung, K. J. Lee, *Nano Lett.* **2014**, *14*, 7031.

Adv. Mater. **2016**,
DOI: 10.1002/adma.201504299

[121] S. Kim, M. K. Gupta, K. Y. Lee, A. Sohn, T. Y. Kim, K.-S. Shin, D. Kim, S. K. Kim, K. H. Lee, H.-J. Shin, D.-W. Kim, S.-W. Kim, *Adv. Mater.* **2014**, *26*, 3918.
[122] B. N. Chandrashekar, B. Deng, A. S. Smitha, Y. Chen, C. Tan, H. Zhang, H. Peng, Z. Liu, *Adv. Mater.* **2015**, DOI:10.1002/adma.201502560.
[123] S. Hana, K. Lee, T. Kim, W. Seung, S. Lee, S. Choi, B. Kumar, R. Bhatia, H. Shin, W. Lee, S. Kim, H. Kim, J. Choi, S. Kim, *Nano Energy* **2015**, *12*, 556.
[124] S. Park, H. Kim, M. Vosgueritchian, S. Cheon, H. Kim, J. H. Koo, T. R. Kim, S. Lee, G. Schwartz, H. Chang, Z. Bao, *Adv. Mater.* **2014**, *26*, 7324.
[125] W. Li, J. Sun, M. Chen, *Nano Energy* **2014**, *3*, 95.
[126] V. Panchal, R. Pearce, R. Yakimova, A. Tzalenchuk, O. Kazakova, *Sci. Rep.* **2013**, *3*, 2597.
[127] J. Cazaux, *Appl. Phys. Lett.* **2011**, *98*, 013109.
[128] K. Y. Lee, J. Chun, J. Lee, K. N. Kim, N. Kang, J. Kim, M. H. Kim, K. Shin, M. K. Gupta, J. M. Baik, S. Kim, *Adv. Mater.* **2014**, *26*, 5037.
[129] Q. Zhong, J. Zhong, B. Hu, Q. Hu, J. Zhou, Z. L. Wang, *Energy Environ. Sci.* **2013**, *6*, 1779.
[130] P. Yang, Z. Lin, Z. L. Wang, K. C. Pradel, L. Lin, X. Li, X. Wen, J. He, Z. L. Wang, *ACS Nano* **2015**, *9*, 901.
[131] X. Zhang, M. Han, R. Wang, B. Meng, F. Zhu, X. Sun, W. Hu, W. Wang, Z. Li, *Nano Energy* **2014**, *4*, 123.
[132] S. Wang, Y. Xie, S. Niu, L. Lin, C. Liu, Y. S. Zhou, Z. L. Wang, *Adv. Mater.* **2014**, *26*, 6720.
[133] S. Wang, Z. Lin, S. Niu, L. Lin, Y. Xie, K. C. Pradel, Z. L. Wang, *ACS Nano* **2013**, *7*, 11263.
[134] X. Pu, L. Li, H. Song, C. Du, Z. Zhao, C. Jiang, G. Cao, W. Hu, Z. L. Wang, Z. L. Wang, *Adv. Mater.* **2015**, *27*, 2472.
[135] S. Jung, J. Lee, T. Hyeon, M. Lee, D. Kim, *Adv. Mater.* **2014**, *26*, 6329.
[136] T. Huang, C. Wang, H. Yu, H. Wang, Q. Zhang, M. Zhu, *Nano Energy* **2015**, *14*, 226.
[137] K. Lee, M. Gupta, S. Kim, *Nano Energy* **2015**, *14*, 139.
[138] G. Zhu, P. Bai, J. Chen, Z. L. Wang, *Nano Energy* **2013**, *2*, 688.
[139] B. Meng, W. Tang, X. Zhang, M. Han, W. Liu, H. Zhang, *Nano Energy* **2013**, *2*, 1101.
[140] W. Tang, C. B. Han, C. Zhang, Z. L. Wang, *Nano Energy* **2014**, *9*, 121.
[141] C. Han, C. Zhang, W. Tang, X. Li, Z. L. Wang, *Nano Res.* **2014**, *8*, 722.
[142] G. Zhu, B. Peng, J. Chen, Q. Jing, Z. L. Wang, *Nano Energy* **2015**, *14*, 126.
[143] P. Bai, G. Zhu, Q. Jing, J. Yang, J. Chen, Y. Su, J. Ma, G. Zhang, Z. L. Wang, *Adv. Funct. Mater.* **2014**, *24*, 5807.
[144] L. Valentini, M. Cardinali, J. Kenny, *J. Polym. Sci., Part B: Polym. Phys* **2014**, *52*, 859.
[145] Y. Yang, H. Zhang, Z. Lin, Y. S. Zhou, Q. Jing, Y. Su, J. Yang, J. Chen, C. Hu, Z. L. Wang, *ACS Nano* **2013**, *7*, 9213.
[146] J. Chen, G. Zhu, J. Yang, Q. Jing, P. Bai, W. Yang, X. Qi, Y. Su, Z. L. Wang, *ACS Nano* **2015**, *9*, 105.
[147] J. Yang, J. Chen, Y. Su, Q. Jing, Z. Li, F. Yi, X. Wen, Z. Wang, Z. L. Wang, *Adv. Mater.* **2015**, *27*, 1316.
[148] F. Yi, L. Lin, S. Niu, P. K. Yang, Z. Wang, J. Chen, Y. Zhou, Y. Zi, J. Wang, Q. Liao, Y. Zhang, Z. L. Wang, *ACS Nano* **2015**, *25*, 3688.
[149] Q. Zheng, B. Shi, F. Fan, X. Wang, L. Yan, W. Yuan, S. Wang, H. Liu, Z. Li, Z. L. Wang, *Adv. Mater.* **2014**, *26*, 5851.
[150] W. Tang, J. Tian, Q. Zheng, L. Yan, J. Wang, Z. Li, Z. L. Wang, *ACS Nano* **2015**, *9*, 7867.
[151] R. Hinchet, S. Kim, *ACS Nano* **2015**, *9*, 7742.
[152] C. Xu, X. D. Wang, Z. L. Wang, *J. Am. Chem. Soc.* **2009**, *131*, 5866.
[153] C. Xu, C. F. Pan, Y. Liu, Z. L. Wang, *Nano Energy* **2012**, *1*, 259.
[154] Y. Yang, Z. L. Wang, *Nano Energy* **2015**, *14*, 245.
[155] M. D. Han, X. S. Zhang, B. Meng, W. Liu, W. Tang, X. M. Sun, W. Wang, H. X. Zhang, *ACS Nano* **2013**, *7*, 8554.
[156] W. S. Jung, M. G. Kang, H. G. Moon, S. H. Baek, S. J. Yoon, Z. L. Wang, S. W. Kim, C. Y. Kang, *Sci. Rep.* **2015**, *5*, 9309.
[157] J. H. Lee, K. Y. Lee, M. K. Gupta, T. Y. Kim, D. Y. Lee, J. Oh, C. Ryu, W. J. Yoo, C. Y. Kang, S. J. Yoon, J. B. Yoo, S. W. Kim, *Adv. Mater.* **2014**, *26*, 765.
[158] D. Choi, K. Y. Lee, M. J. Jin, S. G. Ihn, S. Yun, X. Bulliard, W. Choi, S. Y. Lee, S. W. Kim, J. Y. Choi, J. M. Kim, Z. L. Wang, *Energy Environ. Sci.* **2011**, *4*, 4607.
[159] Y. Yang, H. L. Zhang, G. Zhu, S. Lee, Z. H. Lin, Z. L. Wang, *ACS Nano* **2013**, *7*, 785.